Check for updates

Received: 24 February 2021 | Revised: 11 October 2021 | Accepted: 18 October 2021

DOI: 10.1111/bph.15730

Themed Issue: Advances in Opioid Pharmacology at the Time of the Opioid Epidemic

THEMED ISSUE ARTICLE

Regulator of G-Protein Signalling 4 (RGS4) negatively modulates nociceptin/orphanin FQ opioid receptor signalling: Implication for L-Dopa-induced dyskinesia

Clarissa A. Pisanò[1] | Daniela Mercatelli[1] | Martina Mazzocchi[2] | Alberto Brugnoli[1] | Ilaria Morella[3] | Stefania Fasano[3] | Nurulain T. Zaveri[4] | Riccardo Brambilla[3,5] | Gerard W. O'Keeffe[2] | Richard R. Neubig[6] | Michele Morari[1]

[1]Department of Neuroscience and Rehabilitation, University of Ferrara, Ferrara, Italy

[2]Department of Anatomy and Neuroscience, University College Cork, Cork, Ireland

[3]Neuroscience and Mental Health Research Institute, Division of Neuroscience, School of Biosciences, Cardiff University, Cardiff, UK

[4]Astraea Therapeutics, Medicinal Chemistry Division, Mountain View, California, USA

[5]Department of Biology and Biotechnology "L. Spallanzani", University of Pavia, Pavia, Italy

[6]Department of Pharmacology and Toxicology, Michigan State University, East Lansing, Michigan, USA

Correspondence
Michele Morari, PhD, Department of Neuroscience and Rehabilitation, University of Ferrara, via Fossato di Mortara 17–19, 44121 Ferrara, Italy.
Email: m.morari@unife.it

Funding information
Università degli Studi di Ferrara, Grant/Award Number: FAR1891100

[Correction added on 17 May 2022, after first online publication: CRUI funding statement has been added.]

Background and Purpose: Regulator of G-protein signalling 4 (RGS4) is a signal transduction protein that accelerates intrinsic GTPase activity of $G\alpha_{i/o}$ and $G\alpha_q$ subunits, suppressing GPCR signalling. Here, we investigate whether RGS4 modulates nociceptin/orphanin FQ (N/OFQ) opioid (NOP) receptor signalling and if this modulation has relevance for L-Dopa-induced dyskinesia.

Experimental Approach: HEK293T cells transfected with NOP, NOP/RGS4 or NOP/RGS19 were challenged with N/OFQ and the small-molecule NOP agonist AT-403, using D1-stimulated cAMP levels as a readout. Primary rat striatal neurons and adult mouse striatal slices were challenged with either N/OFQ or AT-403 in the presence of the experimental RGS4 chemical probe, CCG-203920, and D1-stimulated cAMP or phosphorylated extracellular signal regulated kinase 1/2 (pERK) responses were monitored. In vivo, CCG-203920 was co-administered with AT-403 and L-Dopa to 6-hydroxydopamine hemilesioned rats, and dyskinetic movements, striatal biochemical correlates of dyskinesia (pERK and pGluR1 levels) and striatal RGS4 levels were measured.

Key Results: RGS4 expression reduced NOFQ and AT-403 potency and efficacy in HEK293T cells. CCG-203920 increased N/OFQ potency in primary rat striatal neurons and potentiated AT-403 response in mouse striatal slices. CCG-203920 enhanced AT-403-mediated inhibition of dyskinesia and its biochemical correlates, without compromising its motor-improving effects. Unilateral dopamine depletion caused bilateral reduction of RGS4 levels, which was reversed by L-Dopa. L-Dopa acutely up-regulated RGS4 in the lesioned striatum.

Conclusions and Implications: RGS4 physiologically inhibits NOP receptor signalling. CCG-203920 enhanced NOP responses and improved the antidyskinetic potential of

Abbreviations: 6-OHDA, 6-hydroxydopamine; AIMs, abnormal involuntary movements; ALO, axial, limb and orolingual; DA, dopamine; DARPP-32, dopamine and cAMP-regulated phosphoprotein 32 kDa; ERK, extracellular signal regulated kinase 1 and 2; L -Dopa, levodopa; LID, levodopa-induced dyskinesia; MSNs, medium-sized spiny neurons; N/OFQ, nociceptin/orphanin FQ; NOP, nociceptin/orphanin FQ opioid peptide; PD, Parkinson's disease; RGS4, regulator of G-protein signal 4; δ, δ opioid peptide; κ, κ opioid peptide; μ, μ opioid peptide.

This is an open access article under the terms of the Creative Commons Attribution-NonCommercial License, which permits use, distribution and reproduction in any medium, provided the original work is properly cited and is not used for commercial purposes.
© 2021 The Authors. *British Journal of Pharmacology* published by John Wiley & Sons Ltd on behalf of British Pharmacological Society.

NOP receptor agonists, mitigating the effects of striatal RGS4 up-regulation occurring during dyskinesia expression.

LINKED ARTICLES: This article is part of a themed issue on Advances in Opioid Pharmacology at the Time of the Opioid Epidemic. To view the other articles in this section visit http://onlinelibrary.wiley.com/doi/10.1111/bph.v180.7/issuetoc

KEYWORDS
AT-403, CCG-203920, dyskinesia, L-Dopa, nociceptin/orphanin FQ, RGS4

1 | INTRODUCTION

Regulators of G-protein signalling (**RGS**) are signal transduction proteins that couple to heterotrimeric **GPCRs**. RGS proteins bind to the Gα-GTP complex and accelerate its intrinsic GTPase activity, promoting the formation of Gα-GDP and the reassembly of Gαβγ trimer. This causes the termination of GPCR-driven intracellular signalling (Berman et al., 1996; Tesmer et al., 1997). RGS proteins are grouped into five subfamilies (R4, R7, R12, RA and RZ) based on sequence homology. They interact with $G\alpha_i$, $G\alpha_o$, $G\alpha_{12/13}$ but not $G\alpha_s$ and show a variable degree of receptor and G-protein specificity (Kimple et al., 2011; Sjogren, 2017). Different subtypes of RGS have been shown to modulate **opioid receptors** (Traynor, 2012) and have been proposed as novel therapeutic targets for pain, depression and addiction (Gross et al., 2019; Sakloth et al., 2020; Senese et al., 2020; Stratinaki et al., 2013; Traynor & Neubig, 2005). In particular, RGS type 4 (**RGS4**) has been shown to regulate **μ opioid** (Xie et al., 2005) and **δ opioid** (Dripps et al., 2017) receptors, RGS type 9 isoform 2 (**RGS9-2**) regulates μ opioid receptors (Garzon et al., 2001; Psifogeorgou et al., 2007; Zachariou et al., 2003) and RGS type 12 (**RGS12**) regulates **κ opioid** receptors (Gross et al., 2019). Preliminary in vitro evidence suggests that RGS type 19 (**RGS19**) modulates the nociceptin/orphanin FQ opioid (**NOP**) receptor (Xie et al., 2005). The NOP receptor is a 'non-opioid' member of the opioid receptor family, endogenously activated by its natural heptadecapeptide ligand nociceptin/orphanin FQ (**N/OFQ**). N/OFQ regulates several central and peripheral functions (Toll et al., 2016) and is involved in motor disorders, such as Parkinson's disease (**PD**) and **L-Dopa**-induced dyskinesia (LID) (Mercatelli et al., 2020), a major disabling complication of L-Dopa pharmacotherapy of PD (Bastide et al., 2015). Specifically, NOP receptor antagonists proved effective in attenuating motor symptoms and neuropathology associated with experimental parkinsonism, whereas NOP receptor agonists proved effective as antidyskinetic agents in animal models of LID (Arcuri et al., 2018; Marti et al., 2012). However, small-molecule NOP receptor agonists also produced strong hypolocomotion/sedation, which partly masked their antidyskinetic effects (Arcuri et al., 2018). Therefore, in view of the fact that RGS can modulate specific behavioural outcomes of δ opioid and μ opioid receptor stimulation (Dripps et al., 2017), we hypothesized that targeting RGS4 would improve the antidyskinetic effects of NOP receptor agonists relative to their hypolocomotive/sedative effects, which would widen their safety window. In the present study, we investigated the interaction of NOP with a specific subtype of RGS, namely, RGS4, and its relevance for LID in vivo. RGS4 and NOP receptor are expressed in brain areas relevant to LID, such as cortex, striatum and substantia nigra (Ebert et al., 2006; Gold et al., 1997; Neal et al., 1999). Moreover, both RGS4 and NOP are expressed by medium-sized GABAergic striatal neurons, which are the main neurobiological substrate of LID (Ebert et al., 2006; Neal et al., 1999). RGS4 is involved in LID development and expression, and blockade of RGS4 with an antisense nucleotide improved dyskinesia in a rat model of LID (Ko et al., 2014).

In this study, the functional interaction between RGS4 and NOP receptor was investigated first in a cellular model (HEK293T cells) artificially overexpressing both proteins, then in native tissues, that is, rat primary striatal cultures and striatal slices of adult mouse. In native tissues, the RGS4 selective experimental RGS4 chemical probe **CCG-203920** (Turner et al., 2012) was used to pharmacologically

What is already known

- RGS4 is a signal transduction protein that inactivates signalling at $G\alpha_{i/o}$ and $G\alpha_q$-coupled GPCRs.
- RGS4 reduces signalling by μ and δ opioid receptors.

What does this study add

- RGS4 inhibits nociceptin/orphanin FQ opioid (NOP) receptor-mediated responses in vitro while RGS4 blockade potentiates them.
- RGS4 blockade potentiates NOP agonist-mediated attenuation of levodopa-induced dyskinesia and its neurochemical correlates.

What is the clinical significance

- RGS4 inhibitors could potentiate antidyskinetic activity of NOP receptor agonists and widen their safety window.

14765381, 2023, 7, Downloaded from https://bpspubs.onlinelibrary.wiley.com/doi/10.1111/bph.15730 by UNIVERSITA DI PADOVA Centro di Ateneo per le Bib Ca, Wiley Online Library on [13/10/2025]. See the Terms and Conditions (https://onlinelibrary.wiley.com/terms-and-conditions) on Wiley Online Library for rules of use; OA articles are governed by the applicable Creative Commons License

inhibit RGS4 and potentiate NOP receptor responses. The ability of CCG-203920 to potentiate the inhibitory effect of the potent and selective small-molecule NOP receptor agonist **AT-403** (Arcuri et al., 2018) on LID and its biochemical correlates (i.e., pERK and pGluR1 up-regulation) was then tested in vivo. The levels of RGS4 protein in the dyskinetic striatum, both OFF and ON L-Dopa, were also measured.

2 | METHODS

Studies were designed to generate groups of equal size, using randomization and blinded analysis to comply with the *British Journal of Pharmacology* guidelines (Curtis et al., 2018). Experimental protocols were conducted according to the Directive 2010/63/EU. Animal studies are reported in compliance with the ARRIVE guidelines (Percie du Sert et al., 2020) and with the recommendations made by the *British Journal of Pharmacology* (Lilley et al., 2020).

2.1 | Animal subjects

One hundred and ten male Sprague–Dawley rats (150 g; Charles River Lab, Calco, Lecco, Italy; RGD Cat# 734476, RRID:RGD_734476) were used in this study. Seven naïve rats were kept for Western blot (WB) analysis of RGS4 levels (Figure 7) whereas 103 underwent 6-hydroxydopamine (6-OHDA) lesioning. Eighty-five 6-OHDA treated rats passed the selection criteria (see below): 7 were used for WB studies (Figures 5–7) and 78 underwent chronic treatment with L-Dopa. At the end of L-Dopa treatment, we obtained 59 dyskinetic rats (ALO AIM score ≥ 100), of which 35 were kept for WB studies and 24 for behavioural analysis. Sixteen RGS4 knockout ($RGS4^{-/-}$, RRID:IMSR_JAX:005833) backcrossed on C57BL/6J and 16 C57BL/6J wild-type male mice (24–26 g, 10–12 weeks old; RRID:IMSR_JAX:000664) were used for the analysis of RGS4 selectivity of CCG-203920 and RGS4 antibody specificity (Figure S1). Specifically, 10 $RGS4^{-/-}$ mice and 10 C57BL/6J wild-type controls were used for behavioural studies with CCG-203920, and other 6 $RGS4^{-/-}$ mice and 6 C57BL/6J controls were used for WB analysis. C57BL/6J $RGS4^{-/-}$ mice, originally developed by Dr S Heximer (University of Toronto) (Cifelli et al., 2008), were provided by Dr RR Neubig and this colony was raised at the University of Ferrara. Animals were housed in a specific pathogen-free (SPF) standard facility (LARP) of the University of Ferrara with free access to food (4RF21 standard diet; Mucedola, Settimo Milanese, Milan, Italy) and water and kept under regular lighting conditions (12-h dark/light cycle). Animals were housed in groups with environmental enrichments. Adequate measures were taken to minimize animal pain and discomfort. Rats were killed with an overdose of isoflurane or with isoflurane anaesthesia followed by decapitation (WB studies), mice with isoflurane anaesthesia followed by cervical dislocation. Experimental protocols were approved by the Ethical Committee of the University of Ferrara and the Italian Ministry of Health (Licences 714/2016-PR and 368/2018).

Ten time-mated pregnant female Sprague–Dawley rats were used to generate primary cultures of the striatum. They were housed in the Biological Service Unit, at University College Cork under regular conditions of lights (12-h light/dark cycle) with ad libitum access to food and water. On embryonic day (E) 14, embryos (106 in total) were removed by laparotomy from killed dams and used to generated primary cultures of the rat striatum as outlined below (Licence AE19130/I304). Seven 12-week-old male C57BL6 mice were used for **ERK** studies in slices in vitro. Mice were housed in a standard facility at Cardiff University, under regular conditions of light (12-h light/dark cycle), with food and water ad libitum.

2.2 | In vitro experiments

2.2.1 | Cell culture and transfection

HEK cells (HEK293T; ECACC Cat# 12022001, RRID:CVCL_0063) were maintained in a humidified incubator at 37°C with 5% CO_2 and grown to 90%–95% confluence in DMEM supplemented with 10% FBS, 100 $U \cdot ml^{-1}$ penicillin and 100 $\mu g \cdot ml^{-1}$ streptomycin. Cells were transfected with the D1 dopamine (DA) receptor (1 ng per well), $G\alpha_s$ (0.1 ng per well) and NOP (1 ng per well) using Lipofectamine 2000 according to the manufacturer's recommended protocol. All transfections were performed under serum-free conditions in Opti-MEM. Transfections were allowed to proceed for 4–5 h before the media were changed back to DMEM with 10% FBS. Experiments were run 24 h after transfection. For cAMP assays, cells were plated in 6-mm dishes. DNA was kept constant at 6 μg and 6 μl of Lipofectamine 2000 per plate was used. Empty vector (pcDNA3.1+, RRID:Addgene_10842) was used to adjust the total amount of DNA. The lack of cAMP stimulation in control vector (pcDNA3.1+) transfected cells and the robust change in cAMP levels in D1/NOP transfected cells after treatment with specific ligands were used to establish the success of transfection (Feng et al., 2017). This is possible because HEK293T cells do not natively express D1 and NOP receptors.

2.2.2 | cAMP measurements in HEK293T cells

LANCE Ultra cAMP assays (Perkin Elmer; Waltham, MA, USA) were performed in accordance with the manufacturer's instructions. Briefly, the day before the assay, HEK293T cells were transfected as indicated above. On the day of experiment, cells were dissociated from dishes using Versene 1M. Then cells (2000 cells per well in 5 μl) were transferred to a white 384-well microplate (Perkin Elmer) and incubated with various concentrations of N/OFQ and **SKF-38393** (D1 receptor agonist; final 40 nM; 5 μl per well) for 30 min at room temperature. A cAMP standard curve was generated in triplicate according to the manual. Finally, europium (Eu)-cAMP tracer (5 μl) and ULight™-anti-cAMP (5 μl) were added to each well and incubated for 1 h at room temperature. The plate was read on a TR-FRET microplate reader (Synergy NEO; Biotek, Winooski, VT, USA).

14765381, 2023, 7, Downloaded from https://bpspubs.onlinelibrary.wiley.com/doi/10.1111/bph.15730 by UNIVERSITA DI PADOVA Centro di Ateneo per le Bib Ca, Wiley Online Library on [13/10/2025]. See the Terms and Conditions (https://onlinelibrary.wiley.com/terms-and-conditions) on Wiley Online Library for rules of use; OA articles are governed by the applicable Creative Commons License

2.2.3 | ERK measurement in vitro

Adult male C57BL/6J mice were decapitated after anaesthesia and cervical dislocation, and brain slices were freshly prepared according to the protocol previously described (Arcuri et al., 2018; Marti et al., 2012). The brains were rapidly removed and put on a cool glass plate filled with ice-cold sucrose-based dissecting solution (87-mM NaCl, 2.5-mM KCl, 7-mM $MgCl_2$, 1-mM NaH_2PO_4, 75-mM sucrose, 25-mM $NaHCO_3$, 10-mM D-glucose, 0.5-mM $CaCl_2$, 2-mM kynurenic acid), carbogenated (95% O_2, 5% CO_2) and subsequently mounted on the vibratome stage (Vibratome, VT1000S-Leica Microsystems); 200-μm-thick slices were cut and transferred into a brain slice chamber (Brain Slice Chamber-BSC1, Scientific System Design Inc., Mississauga, ON, Canada) and allowed to recover for 1 h at 32°C, with a constant perfusion of carbogenated artificial CSF (ACSF: 124-mM NaCl, 5-mM KCl, 1.3-mM $MgSO_4$, 1.2-mM NaH_2PO_4, 25-mM $NaHCO_3$, 10-mM D-glucose, 2.4-mM $CaCl_2$). The D1 receptor agonist SKF-38393 (100 μM) was applied for 10 min in the presence of AT-403 (30 nM), CCG203920 (500 nM) or vehicle. After fixation in 4% paraformaldehyde (PFA) for 15 min at room temperature, slices were rinsed three times in PBS and cryoprotected in 30% sucrose solution overnight at 4°C. On the following day, slices were further cut into 18-μm-thick slices using a cryostat (Leica CM1850) and mounted onto SuperFrost Plus slides (Thermo Fisher Scientific). Immunohistochemistry was performed as previously described (Papale et al., 2016): 1 h after blocking in 5% normal goat serum and 0.1% Triton X-100 solution, slices were incubated overnight at 4°C with anti-phospho-p44/42 MAPK (Thr202/Tyr204) (Cell Signaling Technology Cat# 4370 RRID:AB_2315112, 1:1000). Sections were then incubated with biotinylated goat anti-rabbit IgG (1:200, Vector Laboratories, Cat# BA 1000 RRID:AB_2313606) for 2 h at room temperature. Detection of the bound antibodies was carried out using a standard peroxidase-based method (Vectastain Elite ABC kit Cat# PK-7100, RRID:AB_2336827, Vector Laboratories), followed by a 3,3′-diamino-benzidine (DAB) and H_2O_2 solution. Images were acquired from the striatum at 40× magnification using a brightfield microscope (Leica Macro/Micro Imaging System), and the number of pERK positive cells in the striatum was counted in each slice.

2.2.4 | Primary striatal neuron cultures

Primary cultures of embryonic (E) day 14 rat ganglionic eminence (hereafter referred to as striatum) (from the Biological Service Unit, University College Cork) were dissected as previously described (Schmidt et al., 2012). All scientific procedures were performed under a licence in accordance with the European Communities Council Directive (86/609/EEC) and approval by local Animal Experimentation Ethics Committee. After dissection, the tissue was dissociated and neurons were plated in poly-D-lysine coated 24-well plates (Sigma) in DMEM:F12 media (Sigma) supplemented with 1% penicillin/streptomycin (Sigma), 1% L-glutamine (Sigma), 2% B27 (Invitrogen) and 1% FBS. Cells were maintained in culture for 7DIV.

2.2.5 | cAMP measurements in primary striatal neurons

On Day 8 of culture, where indicated, cells were treated for 30 min with SKF-38393 (100 μM), CCG-203920 (100 nM) and/or N/OFQ (0.01–1 nM). Cultures were then fixed for 15 min in 4% PFA. Following 3 × 5-min washes in 10-mM PBS-T (0.02% Triton X-100 in 10-mM PBS), cultures were incubated in 5% BSA in 10-mM PBS-T for 1 h at room temperature. Cultures were subsequently incubated in the following primary antibodies: DARPP32 (R and D Systems Cat# AF6259, RRID:AB_10641854; 1:500) and cAMP (R and D Systems Cat# MAB2146, RRID:AB_495027; 1:500), diluted in 1% BSA in 10-mM PBS at 4°C overnight. Following 3 × 5-min washes in 10-mM PBS-T, cells were incubated in 594-conjugated secondary antibodies (Thermo Fisher Scientific Cat# A-11005, RRID:AB_2534073, 1:500) in 1% BSA prior to 3 × 5-min washes. Cells were imaged using an Olympus IX71 inverted microscope. The fluorescence intensity of individual cells was measured by densitometry using ImageJ analysis software (ImageJ, RRID:SCR_003070).

2.3 | In vivo experiments

2.3.1 | Evaluation of RGS4 selectivity of CCG-203920 in mice

As we previously reported (Blazer et al., 2015) that RGS4 inhibitors reverse **raclopride**-induced akinesia in the bar and drag tests (Marti et al., 2004; Viaro et al., 2008), the same tests were used to monitor motor activity in five $RGS4^{-/-}$ mice and five wild-type controls treated with 1 $mg{\cdot}kg^{-1}$ (i.p.) raclopride and, 30 min later, by 10 $mg{\cdot}kg^{-1}$ CCG-203920 or saline (i.p.). Prior to pharmacological testing, mice were trained daily for a week on the behavioural tests until their motor performance became reproducible. The bar (or catalepsy) test measures the ability of the animal to respond to an externally imposed static posture. Each mouse was placed gently on a table and the right and left forepaws were placed alternately on blocks of increasing heights (1.5, 3 and 6 cm). Total time spent on the blocks (in seconds) by each paw was recorded (cut-off time 20 s per block, 60 s maximum) and pooled together. The drag test measures the number of steps made by the animal when gently lifted by the tail (allowing the forepaws on the table) and dragged backward at a constant speed (about 20 $cm{\cdot}s^{-1}$) for a fixed distance (100 cm). The number of steps made by each forepaw was counted by two separate blinded observers and average together.

2.3.2 | Experimental design

A cohort of 10 $RGS4^{-/-}$ mice was allotted in two groups ($n = 5$ each) receiving raclopride followed by CCG-203920 or saline. Four days later, treatments were crossed. The same protocol was adopted for 10 wild-type control mice.

14765381, 2023, 7, Downloaded from https://bpspubs.onlinelibrary.wiley.com/doi/10.1111/bph.15730 by UNIVERSITA DI PADOVA Centro di Ateneo per le Bib Ca, Wiley Online Library on [13/10/2025]. See the Terms and Conditions (https://onlinelibrary.wiley.com/terms-and-conditions) on Wiley Online Library for rules of use; OA articles are governed by the applicable Creative Commons License

2.3.3 | Unilateral 6-OHDA lesion

The unilaterally 6-OHDA lesioned rat, the most popular and best validated rodent model of PD and LID (Cenci & Crossman, 2018; Duty & Jenner, 2011; Schwarting & Huston, 1996), was used. One-hundred three naïve rats (150 g) were unilaterally injected under isoflurane anaesthesia in the (right) medial forebrain bundle with 12 μg of 6-OHDA free base (dissolved in 0.02% ascorbate-saline), according to the following stereotaxic coordinates from bregma and the dural surface (in mm): antero-posterior (AP) −4.4, medio-lateral (ML) 1.2, dorso-ventral (DV) −7.8, tooth bar at −2.4 mm (Paxinos & Watson, 1986), as previously described (Arcuri et al., 2018; Marti et al., 2012; Pisanò et al., 2020). Animals were pretreated with antibiotics (Synulox™, 50 μl·kg^{-1}, i.p.), and the wound was sutured and infiltrated with 2% **lidocaine** solution (Esteve™). Two weeks later, rats were screened by assessing the motor asymmetry score in two different ethological tests (the bar and drag tests) (Marti et al., 2005). Rats showing immobility time > 20 s at the contralateral paw in the bar test and <3 steps at the contralateral paw (or alternatively a contralateral/ipsilateral paw ratio < 50%) were used in the study (Brugnoli et al., 2020; Pisanò et al., 2020).

2.3.4 | L-Dopa treatment and abnormal involuntary movement rating

Seventy-eight rats that successfully passed the threshold values in the bar and drag tests were treated for 21 days with L-Dopa (6 mg·kg^{-1} + **benserazide** 15 mg·kg^{-1}, s.c., once daily) to induce abnormal involuntary movements (AIMs), a correlate of LID (Cenci et al., 1998; Cenci & Lundblad, 2007), as previously described (Brugnoli et al., 2020; Marti et al., 2012; Paolone et al., 2015). Rats were observed for 1 min, every 20 min, during the 3 h that followed L-Dopa injection or until dyskinetic movements ceased. Dyskinetic movements were classified based on their topographical distribution into three subtypes: (i) axial AIM, that is, twisted posture or turning of the neck and upper body towards the side contralateral to the lesion; (ii) forelimb AIM, that is, jerky and dystonic movements and/or purposeless grabbing of the forelimb contralateral to the lesion; and (iii) orolingual AIM, that is, orofacial muscle twitching, purposeless masticatory movements and contralateral tongue protrusion. Each AIM subtype was rated on a frequency scale from 0 to 4 (1, occasional; 2, frequent; 3, continuous but interrupted by an external distraction; 4, continuous and not interrupted by an external distraction). In addition, the amplitude of these AIMs was measured on a scale from 0 to 4 based on a previously validated scale (Cenci & Lundblad, 2007). Axial, limb and orolingual (ALO) AIMs total value was obtained as the sum of the product between amplitude and frequency of each observation (Cenci & Lundblad, 2007), and fully dyskinetic rats scored ≥100.

2.3.5 | Experimental design

Twelve fully dyskinetic rats were randomized to L-Dopa (6 mg·kg^{-1} + benserazide 15 mg·kg^{-1}, s.c.) in combination with AT-403 (0.03 mg·kg^{-1}), CCG-203920 (10 mg·kg^{-1}), AT-403 + CCG-203920 or saline. Each animal was tested four times, with a 3-day washout allowed between treatments. To evaluate whether the potential antidyskinetic effect was associated with an improvement of global motor activity (Arcuri et al., 2018; Marti et al., 2012; Paolone et al., 2015), a separate cohort of 12 rats was subjected to the same treatments as above for the analysis of motor performance on the rotarod, both before (OFF L-Dopa) and after L-Dopa administration (ON L-Dopa). In fact, a truly antidyskinetic compound would alleviate LID and consequently improve rotarod performance whereas a motor inhibiting or a sedative agent would reduce AIMs along with motor performance. Rotarod performance was assessed at 60 min after L-Dopa administration because the ALO AIMs time course showed a peak 60–80 min after L-Dopa administration (Arcuri et al., 2018; Marti et al., 2012; Paolone et al., 2015).

2.3.6 | WB analysis

The Immuno-related procedures used comply with the recommendations made by the *British Journal of Pharmacology* (Alexander et al., 2018). Thirty-five dyskinetic rats were saved for this experiment, but one rat was killed for reaching humane endpoints. Twenty-seven rats were allotted in four groups and treated with L-Dopa alone (6 mg·kg^{-1} + benserazide 15 mg·kg^{-1}, s.c., $n = 6$), or L-Dopa combined with CCG-203920 (10 mg·kg^{-1}, i.p., $n = 7$), AT-403 (0.03 mg·kg^{-1}, $n = 7$) or CCG-203920 + AT-403 ($n = 7$). In combination studies, CCG-203920 was administered first, followed 5 min later by AT-403 and 10 min later by L-Dopa. WB analysis was carried out as previously described (Arcuri et al., 2018; Paolone et al., 2015). Thirty minutes after L-Dopa, rats were anaesthetized with isoflurane, killed by decapitation and striata rapidly dissected and frozen in liquid nitrogen and stored at −80°C until analysis. In the study where RGS4 levels were analysed, seven additional dyskinetic rats (receiving last challenge of L-Dopa 24–48 h earlier) were also included (L-Dopa OFF group). Tissues were homogenized in lysis buffer (SDS 1% buffer, protease inhibitor cocktail and phosphatase inhibitor cocktail) and centrifuged at 18,000× g at 4°C for 15 min. Supernatants were collected, and protein levels were quantified using the Pierce™ BCA protein assay kit (Thermo Fisher Scientific, Cat# 23225). Samples were then stored at −80°C until use. Thirty micrograms of protein per sample were separated on a 4%–12% gradient polyacrylamide precast gels (Bolt® 4%–12% Bis-TrisPlus Gels, Life Technologies) in a Bolt® Mini Gel Tank apparatus (Life Technologies). Proteins were then transferred onto polyvinyldifluoride membrane, blocked for 60 min with 5% non-fat dry milk in 0.1% Tween20 Tris-buffered saline and incubated overnight at 4°C with anti-Thr202/Tyr204-phosphorylated ERK1/2 (pERK) rabbit monoclonal antibody (Merck Millipore, Cat# 05-797R, RRID:AB_1587016, 1:1000), anti-ERK1/2 (totERK) rabbit polyclonal antibody (Merck Millipore Cat# 06-182, RRID:AB_310068, 1:5000), anti-phospho-Ser845 GluR1 (pGluR1) rabbit polyclonal antibody (PhosphoSolutions, Cat# p1160-845, RRID:AB_2492128, 1:1000), anti-glutamate receptor 1 (totGluR1) rabbit polyclonal antibody (Merck Millipore Cat# AB1504, RRID:AB_2113602, 1:1000),

14765381, 2023, 7, Downloaded from https://bpspubs.onlinelibrary.wiley.com/doi/10.1111/bph.15730 by UNIVERSITA DI PADOVA Centro di Ateneo per le Bib Ca, Wiley Online Library on [13/10/2025]. See the Terms and Conditions (https://onlinelibrary.wiley.com/terms-and-conditions) on Wiley Online Library for rules of use; OA articles are governed by the applicable Creative Commons License

anti-TH rabbit monoclonal antibody (Merck Millipore, Cat# AB152, RRID:AB_390204, 1:1000) and anti-α-tubulin rabbit monoclonal antibody (Merck Millipore, Cat# 04-1117, RRID:AB_11213819, 1:25,000). Membranes were washed and then incubated 1 h at room temperature with HRP-linked secondary antibodies (Merck Millipore, Cat# 12-348, RRID:AB_390191, 1:2000). Immunoreactivity was visualized by enhanced chemiluminescence detection kit (Thermo Fisher Scientific, Cat# 32209), and images were acquired using the ChemiDoc MP System quantified using the Image Lab Software (Bio-Rad). Membranes were then stripped and re-probed with rabbit monoclonal anti-α-tubulin antibody (Merck Millipore, Cat# 04-1117, 1:50,000). Data were analysed by densitometry, and the OD of specific total ERK, total GluR1, RGS4 or TH bands was normalized to the corresponding tubulin levels. OD of specific pERK and pGluR1 bands was normalized on totERK and totGluR1 levels, respectively (Arcuri et al., 2018; Paolone et al., 2015). An MW marker from Bio-Rad (Ca# 1610374) was used to identify the specific bands.

2.4 | Data and analysis

The data and statistical analysis comply with the recommendations of the *British Journal of Pharmacology* on experimental design and analysis in pharmacology (Curtis et al., 2018). Statistical analysis was undertaken only for studies where each group size was at least $n = 5$ of independent values and statistical analysis was done on these independent values. A $n = 3$ group size was adopted for studies on CCG-203920 specificity for RGS4 versus RGS19 presented in Figure S1. Group size was determined based on our previous studies with the protocols adopted (Arcuri et al., 2018; Marti et al., 2012; Paolone et al., 2015; Papale et al., 2016). All data were analysed using GraphPad Prism 8.4.3 (GraphPad; LaJolla, CA, USA, RRID:SCR_002798). cAMP data in Figures 1–3 were calculated as percentage of SKF-38393 stimulation. Concentration–response curves for N/OFQ and AT-403 in cells co-transfected with NOP, NOP/RGS4 and NOP/RGS19 were fitted to non-linear least-square regression to the log (inhibitor) versus response (three parameters) in GraphPad Prism. Potency was expressed as pIC_{50} accompanied by 95% confidence interval in parenthesis. pIC_{50} and E_{max} values in Figure 1 were compared by the Student's *t*-test, two-tailed for unpaired data. pERK data in striatal slices (Figure 3) were analysed using a three-way ANOVA followed by the Bonferroni post hoc test. Immobility time and number of steps (Figure 4) were expressed in absolute values and analysed using two-way repeated measure (RM) ANOVA followed by the Tukey test. Dyskinesia values (Figure 5a) were expressed as ALO score (frequency × amplitude) and were treated using two-way RM ANOVA followed by the Tukey test. Rotarod performance (Figure 5b) was expressed as time on rod (in seconds) and was analysed using the Student's *t*-test (two-tailed for unpaired data). WB values in Figures 6 and 7 were analysed using the Student's *t*-test, two-tailed for unpaired data, comparing the signal in the lesioned versus unlesioned striatum. RGS4 protein levels (Figure 8) were expressed as a ratio to tubulin as housekeeper in absolute values (Figure 8a) or as percentage of unlesioned striatum (Figure 8b). Data in Figure 8a were analysed using one-way ANOVA followed by the Newman–Keuls test whereas data in Figure 8b, which did not pass the normality test, with the Kruskal–Wallis test for non-parametric ANOVA followed by the Dunn test. *P* values < 0.05 were considered statistically significant. When parametric statistics was applied, the post hoc tests were conducted only if *F* value from ANOVA reached $P < 0.05$ and there was no significant variance inhomogeneity. Overall, two outliers (one in Figure 1 and another in Figure 8) were excluded from data analysis and representation using the ROUT test implemented on the GraphPad Prism software. Outliers were indicated in figure legends.

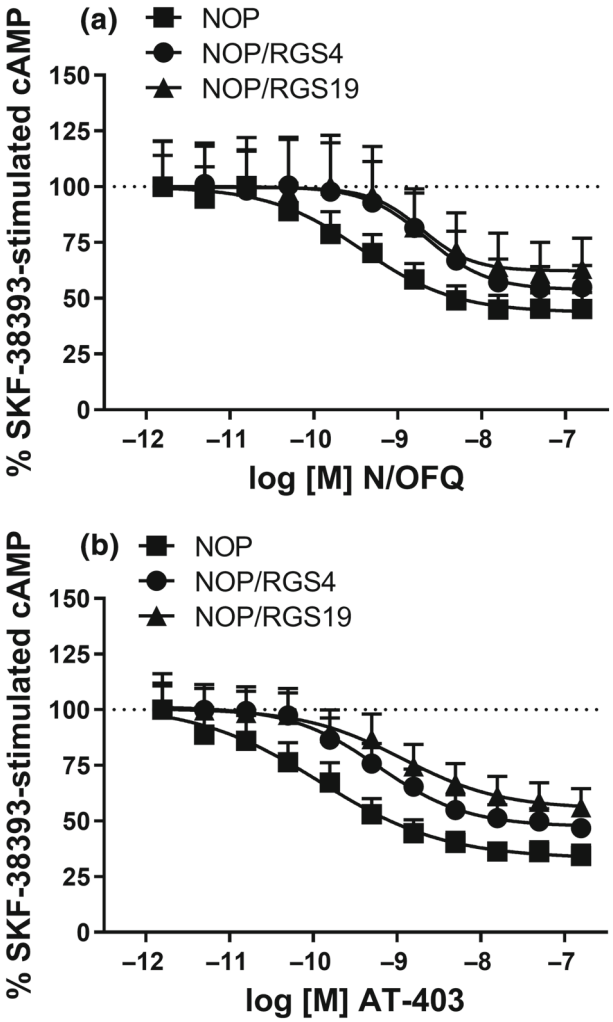

FIGURE 1 RGS4 and RGS19 reduced the NOP receptor agonist ability to attenuate the accumulation of cAMP triggered by D1 receptor agonist in cells. HEK-293T cells were transfected with plasmids for the D1 and NOP receptors, $G\alpha_s$ with or without RGS4 or RGS19 as described in Section 2. They were then stimulated with the D1 receptor agonist SKF-38393 at 40 nM. Concentration–response curves of the NOP receptor agonists N/OFQ (0.001 nM to 1 μM) (a) and AT-403 (0.001 nM to 1 μM) (b). Data are mean ± SEM of $n = 7$ experiments per group (one outlier in the NOP group of panel (b))

14765381, 2023, 7, Downloaded from https://bpspubs.onlinelibrary.wiley.com/doi/10.1111/bph.15730 by UNIVERSITA DI PADOVA Centro di Ateneo per le Bib Ca, Wiley Online Library on [13/10/2025]. See the Terms and Conditions (https://onlinelibrary.wiley.com/terms-and-conditions) on Wiley Online Library for rules of use; OA articles are governed by the applicable Creative Commons License

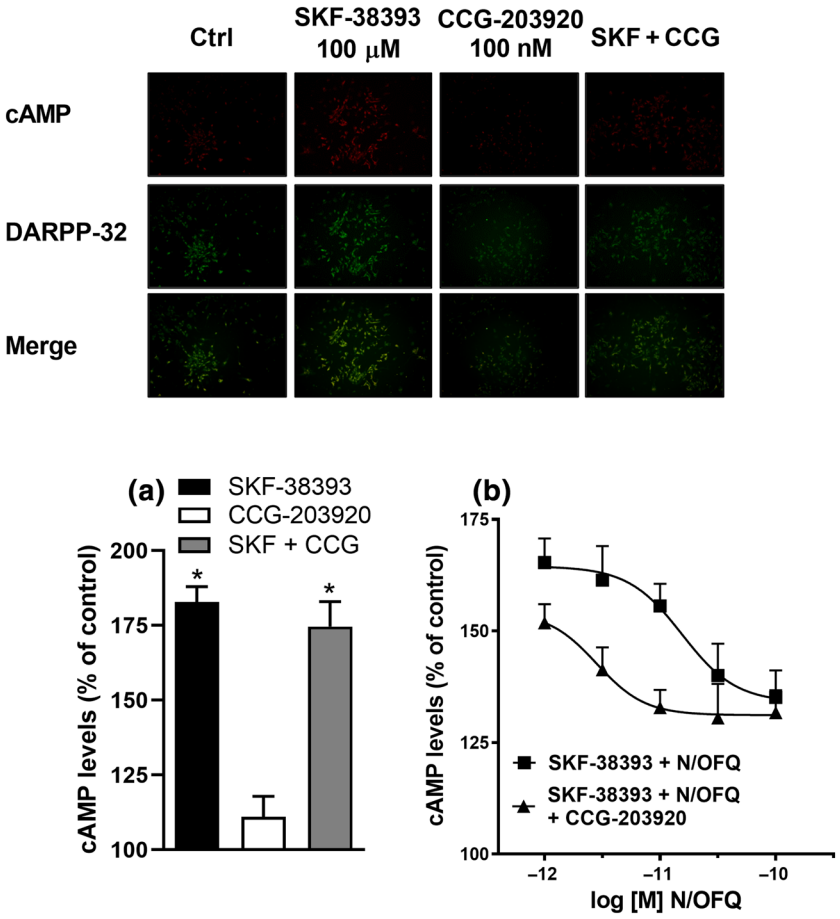

FIGURE 2 RGS4 reduced the NOP receptor agonist ability to attenuate the accumulation of cAMP triggered by D1 receptor agonist in DARPP-32+ striatal primary neurons. DARPP-32 is a marker of MSNs. Neurons were treated with the D1 receptor agonist SKF-38393 (100 μM) and the NOP receptor agonist N/OFQ (0.01–1 nM), in the presence or the absence of the experimental RGS4 chemical probe CCG-203920 (100 nM). (a) Primary effects of SKF-38393, CCG-203920 and their combination, with representative images (upper panels). (b) Concentration–response curves of N/OFQ in the presence or the absence of CCG-203920. Data are mean ± SEM of $n = 8$–10 experiments per group, namely, N/OFQ 0.001 nM $n = 9$, N/OFQ 0.003 nM $n = 8$, N/OFQ 0.01 nM $n = 10$, N/OFQ 0.03 nM $n = 10$ (without CCG-203920) and $n = 8$ (with CCG-203920), N/OFQ 0.1 nM ($n = 9$). $^{*}P < 0.05$, different from CCG-203920 (one-way ANOVA followed by the Bonferroni post hoc test)

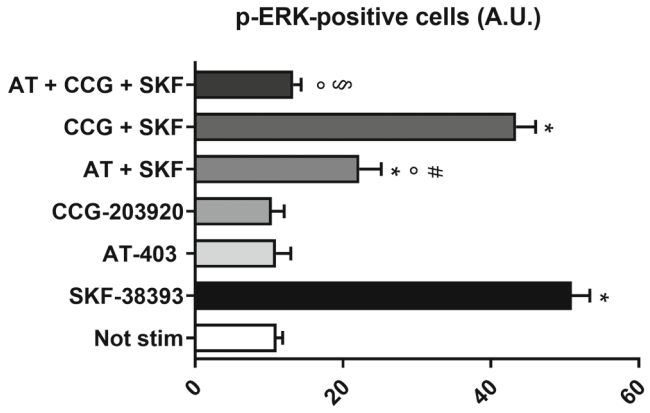

FIGURE 3 CCG-203920 potentiated the AT-403-driven inhibition of D1 receptor-stimulated ERK signalling in striatum. Number of ERK-positive cells in striatal slices of naïve mice following application of the D1 receptor agonist SKF-38393 (100 μM), the NOP receptor agonist AT-403 (30 nM) and the experimental RGS4 chemical probe CCG203920 (50 nM) alone and in combination. Data are mean ± SEM of $n = 7$ mice per group. $^{*}P < 0.05$, different from unstimulated vehicle; $^{\circ}P < 0.05$, different from SKF-38393 alone; $^{\#}P < 0.05$ different from AT-403 alone. $^{\S}P < 0.05$, different from AT-403 + SKF-38393. Three-way ANOVA followed by the Bonferroni post hoc test

2.5 | Materials

AT-403 (2-(1-(1-((1s,4s)-4-isopropylcyclohexyl)piperidin-4-yl)-2-oxoindolin-3-yl)-*N*-methylacetamide) was synthesized by Dr NT Zaveri at Astraea Therapeutics (Mountain View, CA, USA) (Arcuri et al., 2018). **CCG-203920** (4-(2-(methoxyethyl-)-2-ethyl-1,-2,4-thiadiazolidine-3,5-dione) was synthesized by the Medicinal Chemistry Core at Michigan State University (East Lansing, MI, USA). **L-Dopa** methyl ester hydrochloride and **benserazide** hydrochloride were purchased from Sigma-Aldrich (Milan, Italy). 6-OHDA hydrobromide and N/OFQ were purchased from Tocris Bioscience (Bristol, UK). The drug doses or concentrations indicated in text refer to the base form. U1079 antibody was a generous gift of Dr SM Mumby (University of Texas Southwestern, Dallas, TX, USA). AT-403 was dissolved in 2% CH_3COOH 1 M, and 4% DMSO water, L-Dopa, benserazide and CCG-203920 were dissolved in saline and 6-OHDA was dissolved in saline with 0.02% ascorbic acid. N/OFQ and SKF-38393 were dissolved in water. LANCE Ultra cAMP assay was purchased from Perkin Elmer (Waltham, MA, USA). The D1 receptor (Cat# DRD0100000), $G\alpha_s$ (Cat# GNA0SL0000) and NOP (Cat# OPRL100000) plasmids were all purchased from cDNA Resource Center (Bloomsburg, PA, USA).

14765381, 2023, 7, Downloaded from https://bpspubs.onlinelibrary.wiley.com/doi/10.1111/bph.15730 by UNIVERSITA DI PADOVA Centro di Ateneo per le Bib Ca, Wiley Online Library on [13/10/2025]. See the Terms and Conditions (https://onlinelibrary.wiley.com/terms-and-conditions) on Wiley Online Library for rules of use; OA articles are governed by the applicable Creative Commons License

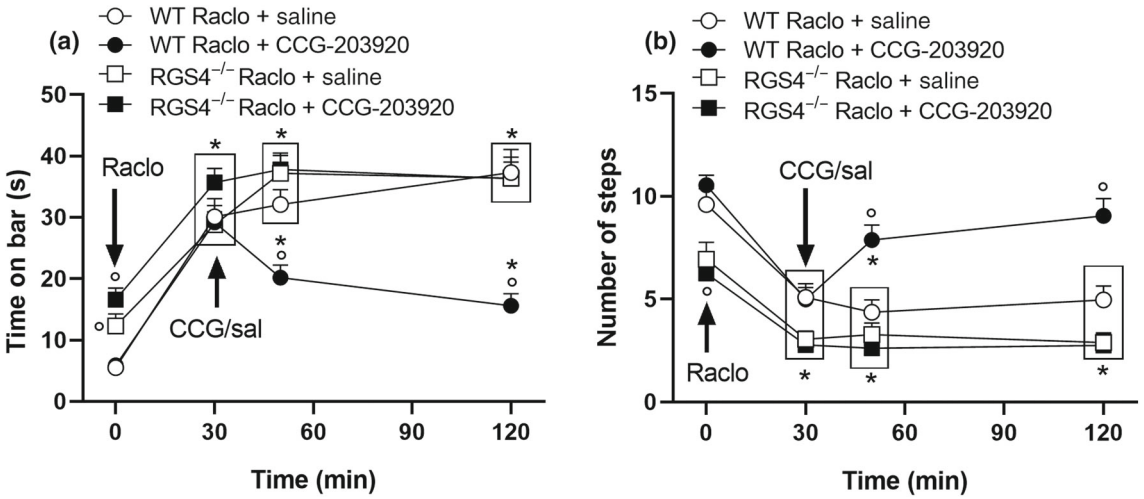

FIGURE 4 CCG-203920 reversed raclopride-induced akinesia in wild-type (WT) but not in RGS4$^{-/-}$ mice. Immobility time in the bar test (in seconds) (a) and number of steps in the drag test (b) were monitored before (baseline, time 0) and after the administration of 1 mg·kg^{-1} of the D2 receptor antagonist raclopride (i.p.), followed 30 min later by the experimental RGS4 chemical probe CCG-203920 10 mg·kg^{-1} or saline (i.p.). Arrows indicate the time of drug administration. Data are mean ± SEM of $n = 10$ determinations per group, obtained from 10 WT and 10 RGS4$^{-/-}$ mice treated under a crossover design. *$P < 0.05$, different from baseline; °$P < 0.05$, different from raclopride in WT mice (two-way RM ANOVA followed by the Tukey post hoc test)

2.6 | Nomenclature of targets and ligands

Key protein targets and ligands in this article are hyperlinked to corresponding entries in http://www.guidetopharmacology.org and are permanently archived in the **Concise Guide to PHARMACOLOGY 2021/22: Introduction and Other Protein Targets** (Alexander, Kelly, et al., 2021) and **Concise Guide to PHARMACOLOGY 2021/22: G protein-coupled receptors** (Alexander, Christopoulos, et al., 2021).

3 | RESULTS

3.1 | In vitro experiments

3.1.1 | RGS4 negatively modulates NOP receptor-driven inhibition of D1-stimulated cAMP production in HEK293T cells

The crosstalk between NOP and RGS4 was first investigated in HEK273 cells by measuring the inhibition of cAMP production stimulated by D1 receptor agonist SKF-38393 (40 nM) as a biochemical readout (Figure 1). The NOP receptor endogenous ligand, N/OFQ, and the small-molecule NOP agonist, AT-403, were tested in cells transfected with the NOP receptor alone or with RGS4. In NOP-transfected cells (Figure 1), N/OFQ inhibited cAMP production in a concentration-dependent manner. N/OFQ showed a pIC$_{50}$ of 9.43 (10.15–8.70) and a maximal inhibition of cAMP production (E$_{max}$) of 61%. Co-transfection of RGS4 with the NOP receptor caused a rightward shift of the concentration–response curve of N/OFQ (Figure 1a) with a significant reduction of pIC$_{50}$ to 8.66 (9.62–7.69) (df = 12, $t = 3.56$) and a non-significant reduction of E$_{max}$ to 45%. To investigate whether the NOP receptor might be regulated by other RGS proteins, the response of N/OFQ in the presence of RGS19 was assessed (Figure 1a). In fact, RGS19 is structurally very similar to RGS4 and was reported to interact with the NOP receptor (Xie et al., 2005). When NOP receptor and RGS19 were co-transfected, the N/OFQ curve was shifted to the right (Figure 1), with a significant reduction of N/OFQ potency (pIC$_{50}$ 8.71, 9.88–7.55) (df = 12, $t = 3.093$) and a non-significant reduction of N/OFQ E$_{max}$ to 39%.

Whether RGS4 and RGS19 also modulate the effect of AT-403 was next investigated. AT-403 (Figure 1b) inhibited the D1-stimulated cAMP production in a concentration-dependent manner, showing slightly higher potency (pIC$_{50}$ = 9.92, 10.78–9.06) and efficacy (75%) than N/OFQ. RGS4 co-transfection caused a rightward shift of the AT-403 curve (Figure 1b), with a significant reduction of potency (pIC$_{50}$ = 9.22, 9.77–8.66) (df = 11, $t = 2.71$) and efficacy (50%, df = 11, $t = 3.79$). Co-transfection of RGS19 also shifted to the right of the AT-403 curve (Figure 1b), leading to a significant reduction (df = 11, $t = 4.10$) of AT-403 potency (pIC$_{50}$ = 8.93, 9.92–7.93) and efficacy (44%, df = 11, $t = 3.24$).

3.1.2 | CCG-203920 potentiated the NOP response in rat primary striatal neurons

To investigate the occurrence of a RGS4–NOP receptor interaction in native tissues, the impact of pharmacological inhibition of RGS4 on NOP responses was investigated using the experimental RGS4 chemical probe CCG-203920 in individual medium-sized spiny neurons (MSNs) in primary cultures of the E14 rat striatum (Figure 2).

14765381, 2023, 7, Downloaded from https://bpspubs.onlinelibrary.wiley.com/doi/10.1111/bph.15730 by UNIVERSITA DI PADOVA Centro di Ateneo per le Bib Ca, Wiley Online Library on [13/10/2025]. See the Terms and Conditions (https://onlinelibrary.wiley.com/terms-and-conditions) on Wiley Online Library for rules of use; OA articles are governed by the applicable Creative Commons License

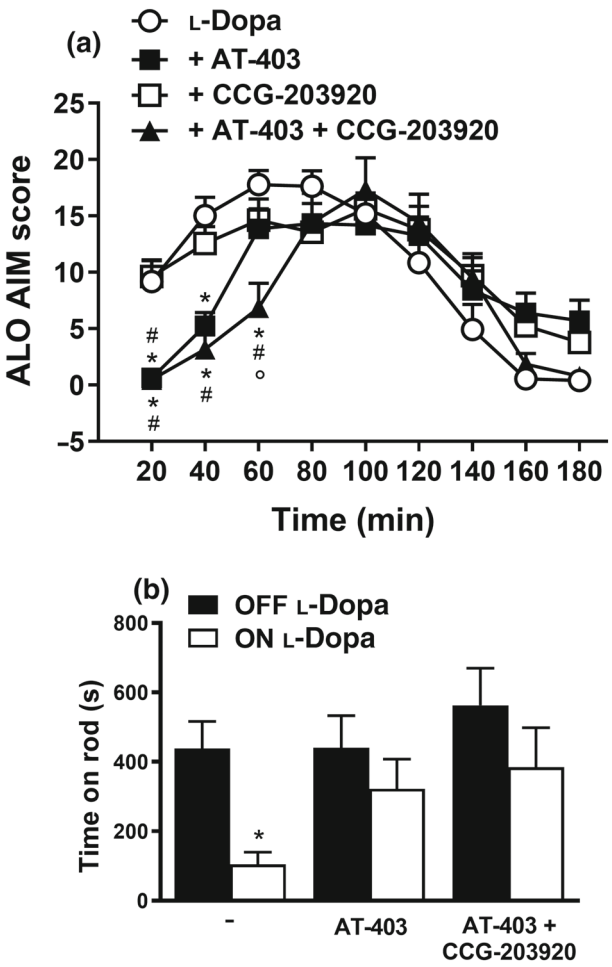

FIGURE 5 CCG-203920 extended the antidyskinetic effect of AT-403 without worsening motor performance on the rotarod. (a) ALO AIMs were scored in 6-OHDA hemilesioned dyskinetic rats following challenge with L-Dopa (6 mg·kg^{-1} plus benserazide 15 mg·kg^{-1}, s.c.) combined with vehicle, the NOP receptor agonist AT-403 (0.03 mg·kg^{-1}, s.c.) or the experimental RGS4 chemical probe CCG-203920 (10 mg·kg^{-1}, i.p.) (a). Values are mean ± SEM of 13 rats per group. *P < 0.05, different from L-Dopa; $^{\#}P$ < 0.05, different from L-Dopa + CCG-203920; °P < 0.05, different from L-Dopa + AT-403. Two-way repeated measure ANOVA followed by the Tukey post hoc test. (b) Rotarod performance was evaluated as time on rod in seconds, before (OFF) and 60 min after (ON) L-Dopa (6 mg·kg^{-1} plus benserazide 15 mg·kg^{-1}, s.c.) combined with vehicle, AT-403 (0.03 mg·kg^{-1}, s.c.) or CCG-203920 (10 mg·kg^{-1}, i.p.). Values are mean ± SEM of 11 rats per group. *P < 0.05, different from OFF L-Dopa (Student's t-test, two-tailed for unpaired data)

CCG-203920 was chosen as the most selective agent for RGS4 versus RGS19, which is also able to modulate NOP effects in HEK-293 cells. Like its close derivative CCG-203769 (compound 11b, while CCG-203920 is compound 13 in Turner et al., 2012), CCG-203920 acts most potently on RGS4 of all RGS proteins tested. Indeed, a preliminary analysis revealed that CCG-203920 is nearly 100-fold selective for RGS4 versus RGS19 (Figure S1) whereas CCG-203769 is 8-fold selective for RGS4 versus RGS19 (Blazer et al., 2015). Individual MSNs were identified using immunocytochemistry for DARPP-32, which is a well-known marker of MSNs (Ouimet et al., 1984), and were co-stained for cAMP. cAMP accumulation was then measured in DARPP32+ neurons stimulated with the D1 receptor agonist SKF-38393 (100 μM) combined with increasing concentrations of N/OFQ, in the presence or the absence of CCG-203920 (100 nM). SKF-38393 caused an 83% increase of cAMP levels that was not significantly affected by CCG-203920 (Figure 2a). N/OFQ inhibited the stimulation induced by SKF-38393 in a concentration-dependent manner with a pIC_{50} of 10.81 (11.36–10.26) and a 70% maximal inhibition of cAMP levels (Figure 2b). CCG-203920 caused a leftward shift of N/OFQ pIC_{50} to 11.55 (12.43–10.67), without changing N/OFQ efficacy (Figure 2b).

3.1.3 | CCG-203920 potentiated NOP response in mouse striatal slices

Relying on the well-established NOP receptor inhibitory activity on D1 signalling (Olianas et al., 2008), we next investigated whether RGS4 could affect the AT-403-mediated inhibition of the SKF-38393-induced ERK-positive cell number in slices of mouse striatum (Figure 3). Application of the D1 receptor agonist SKF-38393 (100 μM) (Arcuri et al., 2018; Fasano et al., 2009; Marti et al., 2012) to striatal slices of naïve mice caused an approximately fourfold increase in the number of pERK immunoreactive cells over basal (three-way ANOVA, $F_{1,42} = 213.909$; Figure 3). AT-403 alone (30 nM) had no effect on basal pERK levels but reduced D1 receptor-mediated response by 56% (three-way ANOVA, $F_{1,42} = 102.746$). CCG-203920, which was ineffective alone, significantly potentiated the effects of AT-403 (three-way ANOVA, $F_{1,42} = 9.222$). In fact, when co-applied with CCG-203920, AT-403 fully inhibited D1 stimulation.

3.2 | In vivo experiments

3.2.1 | CCG-203920 targets RGS4 in vivo

To confirm the RGS4 selectivity of CCG-20920 in vivo, the neuroleptic-induced akinesia/catalepsy model was used because we previously reported that the RGS4 inhibitor CCG-203769 reversed raclopride-induced akinesia in mice (Blazer et al., 2015). RGS4$^{-/-}$ mice were slightly hypokinetic at baseline, showing >2-fold greater immobility time in the bar test (14.45 ± 1.40 s, $n = 20$) and 40% reduced stepping activity in the drag test (6.59 ± 0.56 steps, $n = 20$) compared with controls (5.7 ± 0.48 s and 10.08 ± 0.45 steps, respectively; $n = 20$ each). Two-way ANOVA revealed that raclopride caused a prolonged and marked increase of the immobility time (time $F_{3,108} = 117.3$, $P < 0.05$ treatment $F_{3,36} = 11.34$, $P < 0.05$, time × treatment interaction $F_{9,108} = 6.35$, $P < 0.05$) and a reduction of stepping activity (time $F_{3,95} = 67.50$, $P < 0.05$; treatment $F_{3,36} = 18.95$, $P < 0.05$, time × treatment interaction $F_{9,108} = 4.09$, $P < 0.05$) in both wild-type and RGS4$^{-/-}$ mice (Figure 4).

14765381, 2023, 7, Downloaded from https://bpspubs.onlinelibrary.wiley.com/doi/10.1111/bph.15730 by UNIVERSITA DI PADOVA Centro di Ateneo per le Bib Ca, Wiley Online Library on [13/10/2025]. See the Terms and Conditions (https://onlinelibrary.wiley.com/terms-and-conditions) on Wiley Online Library for rules of use; OA articles are governed by the applicable Creative Commons License

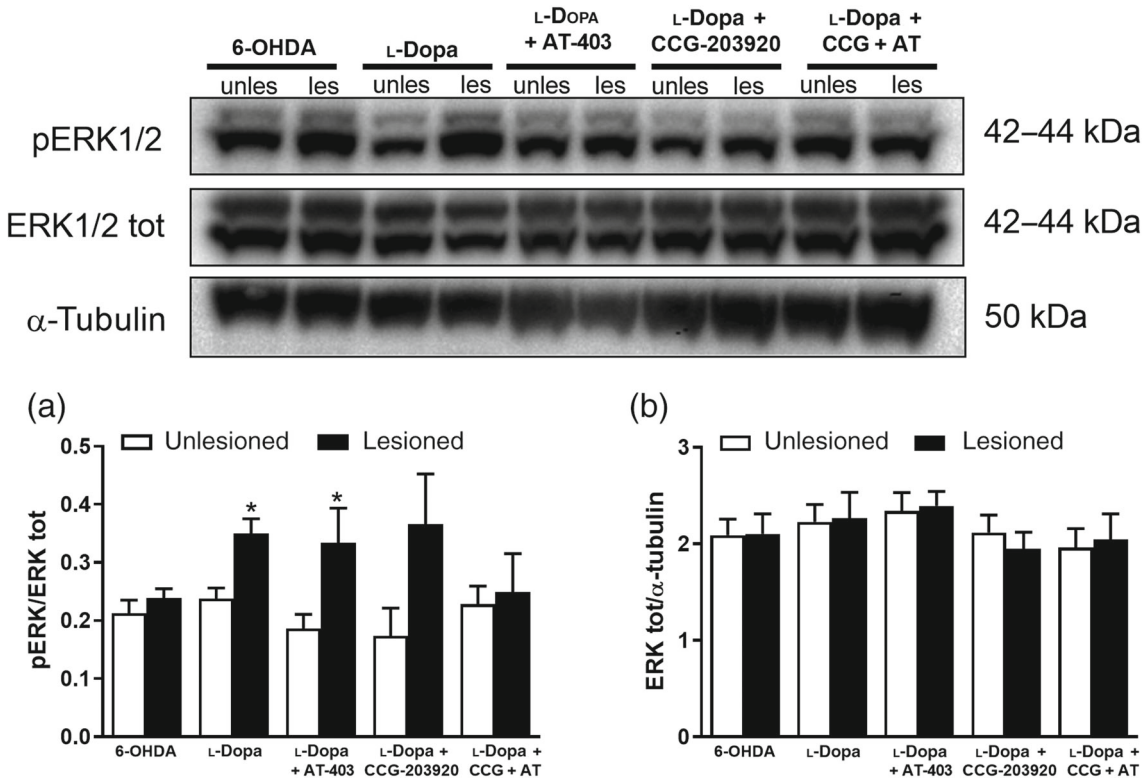

FIGURE 6 AT-403 in combination with CCG-203920 inhibited L-Dopa-induced ERK phosphorylation in the striatum of dyskinetic rats. Western blot representative images (upper panel) and quantification (lower panel) of pERK (a) and total ERK (b) in the lesioned and unlesioned striata of 6-OHDA hemilesioned L-Dopa-naïve or dyskinetic rats. Dyskinetic rats were treated with the NOP receptor agonist AT-403 (0.03 mg·kg^{-1}, s.c.) or vehicle and, 10 min later, challenged with L-Dopa (6 mg·kg^{-1}, i.p.). The experimental RGS4 chemical probe CCG-203920 (10 mg·kg^{-1}, i.p.) or vehicle were administered 5 min before AT-403. Values are mean ± SEM of six rats per group. *P < 0.05, different from unlesioned striatum (Student's t-test, two-tailed for unpaired data)

CCG-203920 administration significantly reversed raclopride-induced hypokinesia in wild-type animals but was ineffective in RGS4$^{-/-}$ mice, suggesting RGS4 targeting at this dose.

3.2.2 | CCG-203920 extended the antidyskinetic effect of AT-403

In a previous study, we described the dose-dependent antidyskinetic effect of AT-403 in the 6-OHDA rat model of LID in vivo (Arcuri et al., 2018). At the highest dose, tested AT-403 (0.1 mg·kg^{-1}) exerted strong sedative effects that overlapped the antidyskinetic effect. Conversely, at the dose of 0.03 mg·kg^{-1}, AT-403 exerted a mild and transient antidyskinetic effect in the absence of sedation. Here, in the same model, to improve the antidyskinetic effect of this AT-403 dose, we challenged AT-403 (0.03 mg·kg^{-1}, s.c.) with L-Dopa (6 mg·kg^{-1} + benserazide 15 mg·kg^{-1}, s.c.) in the presence and in the absence of CCG-203920 10 mg·kg^{-1} (Figure 5a). AT-403 alone delayed the onset of AIMs by 40 min, without affecting the overall duration and severity of the response. Co-administration of CCG-203920 caused a further 20-min delay in AIM appearance, without significantly affecting the overall response to AT-403 (Figure 5a), suggesting that RGS4 blockade potentiates NOP agonist-induced antidyskinetic effects (significant effect of time $F_{8,432} = 37.00$, treatment $F_{3,432} = 6.86$ and time × treatment interaction $F_{24,432} = 43.06$).

3.2.3 | CCG-203920 did not affect the improvement of rotarod performance ON L-Dopa induced by AT-403

To investigate whether CCG-203920 increased the sedative effects along with the antidyskinetic effect of AT-403, the rotarod performance was monitored before (baseline, OFF L-Dopa) and after L-Dopa administration in dyskinetic rats (Arcuri et al., 2018; Marti et al., 2012; Paolone et al., 2015) (Figure 5b). As expected, the time spent on the rod after L-Dopa administration was dramatically reduced compared with baseline due to dyskinetic movement appearance (−76%; df = 10, $t = 4.075$). When animals were pretreated with AT-403, the rotarod performance ON L-Dopa improved and no significant reduction with respect to baseline condition was observed (Figure 5b). CCG-203920 administration did not worsen the motor promoting effect of AT-403, indicating that RGS4 blockade did not potentiate AT-403-induced sedation.

14765381, 2023, 7, Downloaded from https://bpspubs.onlinelibrary.wiley.com/doi/10.1111/bph.15730 by UNIVERSITA DI PADOVA Centro di Ateneo per le Bib Ca, Wiley Online Library on [13/10/2025]. See the Terms and Conditions (https://onlinelibrary.wiley.com/terms-and-conditions) on Wiley Online Library for rules of use; OA articles are governed by the applicable Creative Commons License

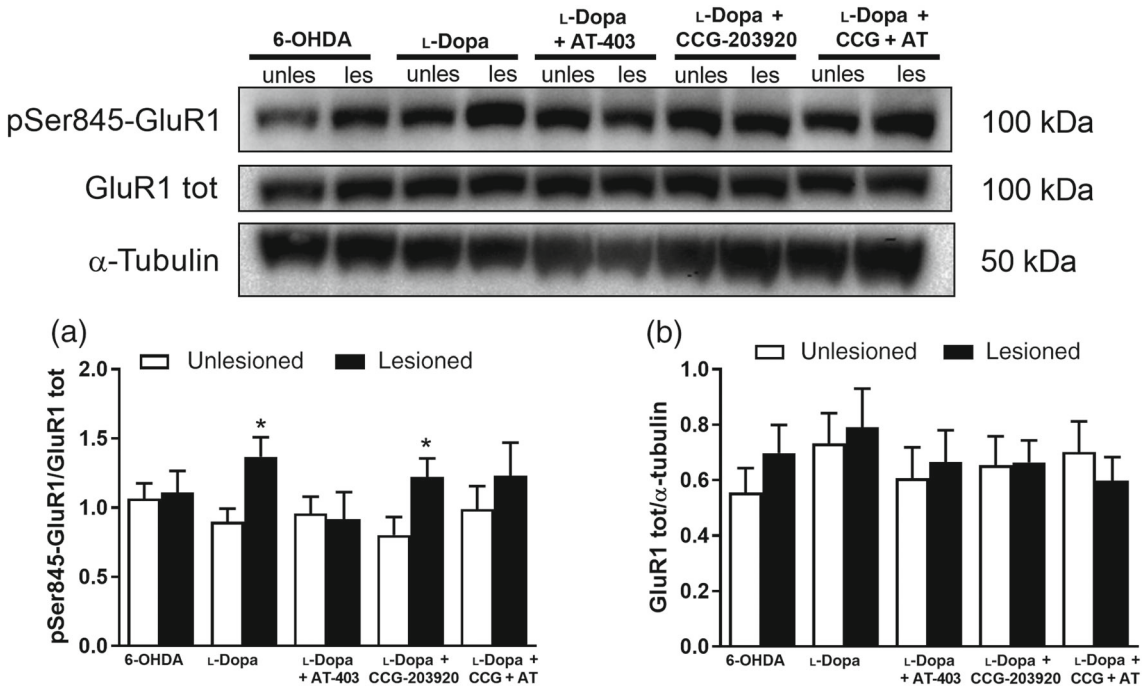

FIGURE 7 AT-403 inhibited the L-Dopa-stimulated pGluR1 phosphorylation in the striatum of dyskinetic rats. Western blot representative images (upper panel) and quantification (lower panel) of pGluR1 (a) and total GluR1 (b) in the striatum of 6-OHDA hemilesioned, L-Dopa-naïve or dyskinetic rats. Dyskinetic rats were treated with the NOP receptor agonist AT-403 (0.03 mg·kg^{-1}, s.c.) or vehicle and, 10 min later, challenged with L-Dopa (6 mg·kg^{-1}, i.p.). The experimental RGS4 chemical probe CCG-203920 (10 mg·kg^{-1}, i.p.) or vehicle were administered 5 min before AT-403. Values are mean ± SEM of six rats per group. *P < 0.05, different from unlesioned striatum (Student's t-test, two-tailed for unpaired data)

3.2.4 | CCG-203920 potentiated the AT-403 inhibition of ERK signalling in striatum

Aberrant D1 receptor transmission in direct pathway MSNs is associated with LID and leads to alterations in phosphorylating activity of several downstream kinases, such as PKA and DARPP-32 (Bastide et al., 2015). A direct consequence of the hyperactivity of DARPP-32 is the increased phosphorylation of ERK1/2, a well-accepted correlate of LID in rodents (Pavon et al., 2006; Santini et al., 2007). In a previous study, we showed that AT-403 (0.1 mg·kg^{-1}) was able to normalize the L-Dopa-induced pERK levels in the 6-OHDA lesioned, DA-depleted striatum (Arcuri et al., 2018). In the present study, we investigated whether a lower dose of AT-403 (0.03 mg·kg^{-1}) alone or in combination with CCG-203920 could normalize L-Dopa-induced increase of pERK in the striatum of dyskinetic rats (Figure 6). As expected, LID was associated with a significant increase of pERK levels in the lesioned striatum relative to the unlesioned striatum (+47%; $t = 3.584$, df = 12), which was unaffected by pretreatment with AT-403 (+79%; $t = 2.261$, df = 10) or CCG-203920 (+117%; significance just above the threshold value $t = 1.947$, df = 10, $P = 0.08$; Figure 6a). However, when L-Dopa was combined with CCG-203920 and AT-403, pERK levels did not rise in the lesioned striatum (Figure 6a). Pharmacological treatments did not affect total protein levels (Figure 6b), suggesting that the changes observed were due to the activation of the pathway and not protein expression.

3.2.5 | AT-403 inhibited D1 receptor-stimulated pGluR1 phosphorylation in striatum

The increase of pGluR1 levels is another biochemical correlate of LID in rodents (Santini et al., 2007). GluR1 is a subunit of the glutamate AMPA receptor, which is physiologically phosphorylated by PKA activated by DA via D1 receptors. We therefore investigated whether CCG-203920 potentiates the ability of AT-403 (0.03 mg·kg^{-1}) to modulate pGluR1 levels. As expected, L-Dopa elevated pGluR1 levels in the lesioned stratum (+52%; $t = 2.272$, df = 12; Figure 7a). However, in contrast to the effect on ERK, AT-403 alone was able to normalize pGluR1 levels (Figure 7a), in line with the well-known inhibitory influence of NOP receptors over canonical D1 signalling. CCG-203920 did not alter the L-Dopa-induced increase (+52%; $t = 2.239$, df = 10) or the AT-403-driven normalization of pGluR1 levels. Again, neither treatment affected total protein amounts (Figure 7b).

3.2.6 | Striatal RGS4 levels were modulated by DA depletion and L-Dopa treatment

To investigate whether RGS4 inhibition corrects a plastic adaptation of RGS4 occurring as a consequence of DA depletion and/or L-Dopa administration (Geurts et al., 2003; Ko et al., 2014), RGS4 levels

14765381, 2023, 7, Downloaded from https://bpspubs.onlinelibrary.wiley.com/doi/10.1111/bph.15730 by UNIVERSITA DI PADOVA Centro di Ateneo per le Bib Ca, Wiley Online Library on [13/10/2025]. See the Terms and Conditions (https://onlinelibrary.wiley.com/terms-and-conditions) on Wiley Online Library for rules of use; OA articles are governed by the applicable Creative Commons License

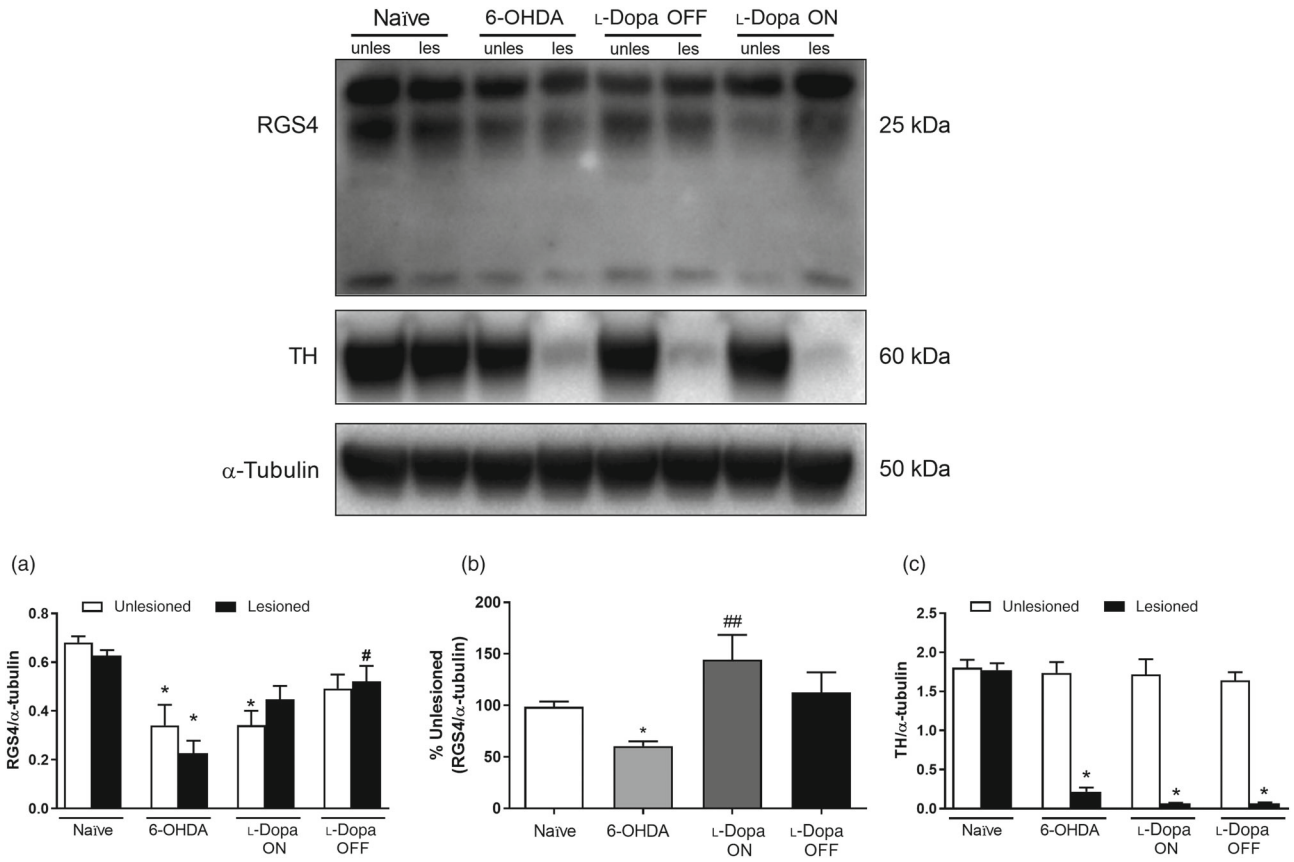

FIGURE 8 RGS4 levels were modulated by 6-OHDA and L-Dopa treatment. Western blot representative images (upper panel) and quantification (lower panel) of RGS4 in the striatum of naïve, 6-OHDA hemilesioned L-Dopa naive or dyskinetic rats. In dyskinetic rats, RGS4 analysis was carried out both OFF and ON L-Dopa. RGS4 values were normalized to α-tubulin as housekeeper and expressed as absolute values (a) or percentage of RGS4 in the lesioned relative to unlesioned striatum (b). TH levels normalized to α-tubulin are also shown (c). Values are mean ± SEM of seven rats per group ($n = 6$ in the ON L-Dopa group due to animal loss; in panel (b), one outlier was removed from the 6-OHDA group). $^{*}P < 0.05$, different from naïve (a,b) or unlesioned striatum (c); $^{\#}P < 0.05$ different from 6-OHDA (b). One-way ANOVA followed by the Newman–Keuls test (a), the Kruskal–Wallis test followed by the Dunn test (b). Student's *t*-test, two-tailed for unpaired data (c)

were measured by Western analysis in the striatum of naïve, L-Dopa naïve 6-OHDA hemilesioned and dyskinetic rats (Figure 8). In dyskinetic rats, RGS4 levels were measured both ON and OFF L-Dopa. The specificity of the antibody used was first confirmed in RGS4$^{-/-}$ mice (Figure S2). ANOVA revealed a strong effect of treatment ($F_{7,46} = 7.95$). A marked decrease in RGS4 protein levels was found in both the lesioned (−64%) and unlesioned (−51%) striata of 6-OHDA animals, when compared with respective naïve counterparts (Figure 8a). If RGS4 levels were expressed as lesioned-to-unlesioned ratio, a significant reduction was detected in 6-OHDA hemilesioned rats compared with naive rats ($H_{3,20} = 13.73$) (Figure 8b). Chronic L-Dopa (OFF group) normalized the ratio. However, acute L-Dopa (ON group) reversed it, causing a 44% increase of RGS4 levels in the lesioned striatum. This suggests that RGS4 is rapidly up-regulated in the lesioned striatum of dyskinetic animals following acute stimulation of aberrant D1 receptor signalling by L-Dopa.

4 | DISCUSSION AND CONCLUSIONS

The present study provides strong evidence that RGS4 inhibits NOP receptor responses in vitro. Moreover, this study demonstrates that pharmacological inhibition of RGS4 potentiates the ability of a NOP agonist to attenuate LID and its neurochemical correlates in vivo, without worsening its sedative properties. These data point to a functional RGS4–NOP receptor interaction and add to previous reports that RGS4 fine-tunes opioid receptor signalling and behaviours (Dripps et al., 2017; Han et al., 2010; Stratinaki et al., 2013; Xie et al., 2005). In fact, RGS4 negatively regulated reward and physical dependence induced by the MOP receptor preferential agonist morphine but did not affect morphine-induced analgesia or tolerance (Han et al., 2010). RGS4 also differentially modulated DOP receptor-mediated behavioural outcomes in mice, because genetic deletion of RGS4 as well as acute pharmacological inhibition of RGS4 with CCG-203769 increased SNC80-induced antinociception and

14765381, 2023, 7, Downloaded from https://bpspubs.onlinelibrary.wiley.com/doi/10.1111/bph.15730 by UNIVERSITA DI PADOVA Centro di Ateneo per le Bib Ca, Wiley Online Library on [13/10/2025]. See the Terms and Conditions (https://onlinelibrary.wiley.com/terms-and-conditions) on Wiley Online Library for rules of use; OA articles are governed by the applicable Creative Commons License

antihyperalgesia but did not affect the pro-convulsant action of this DOP agonist (Dripps et al., 2017; Stratinaki et al., 2013).

The interaction between RGS4 and NOP receptor was originally evaluated in COS-7 cells transfected with a dual-expression plasmid containing RGS4 and each of the opioid receptor subtypes (Xie et al., 2005). In that study, a single concentration of N/OFQ was tested, which was poorly modulated by RGS4. In fact, RGS4 increased by 28% N/OFQ GTPase activity but left unaffected N/OFQ inhibition of forskolin-induced cAMP levels. In the present study in HEK293T cells, RGS4 did not affect N/OFQ efficacy but significantly reduced its potency. Moreover, it reduced both the efficacy and potency of the potent and selective small-molecule agonist AT-403. In NOP-transfected HEK293T cells, N/OFQ and AT-403 inhibited the D1-stimulated cAMP production, a $G_{i/o}$ protein-mediated intracellular function (Feng et al., 2017) with similar potencies (9.43 and 9.92, respectively). These values are consistent with those reported for N/OFQ and AT-403 in the [^{35}S]GTPγS and calcium mobilization assays (Ferrari et al., 2017), confirming that AT-403 is a potent full agonist at the NOP receptor. The rightward shift of N/OFQ and AT-403 curves and the reduction of AT-403 efficacy in the presence of RGS4 suggest that RGS4 negatively couples to $G_{i/o}$ to inhibit NOP receptor signalling. However, this effect is shared by another RGS protein, RGS19, functionally very close to RGS4, which was reported to negatively modulate NOP receptor signalling in vitro (Xie et al., 2005). Interestingly, RGS19 reduced the efficacy of AT-403 but showed only a trend for reduction of N/OFQ efficacy. Thus, RGS4 and RGS19 seem to modulate more efficiently the efficacy of AT-403 than of N/OFQ. This could be due to the different modes of interaction and activation of the NOP receptor by the endogenous ligand N/OFQ versus a small-molecule nonpeptidic ligand like AT-403.

The occurrence of a RGS4–NOP functional interaction was confirmed in native systems, that is, striatal primary neurons and striatal slices, using an experimental RGS4 chemical probe to block the endogenous activity of RGS4. Primary striatal neurons express both RGS4 and NOP (Buzas et al., 1998; Runne et al., 2008) and the two functionally interact to modulate D1 receptor-evoked responses because the highly RGS4-selective CCG-203920 increased N/OFQ potency in inhibiting D1-stimulated cAMP levels. This interaction occurs in DARRP32-positive, likely GABAergic, neurons, indicating that this interaction is not an artefact of protein overexpression in HEK273 cells but is endogenously active and physiologically relevant. This interaction occurs not only in developing tissues in rats but also in adult mice. We previously demonstrated that N/OFQ and AT-403 inhibited the increase of ERK-positive striatal neurons (likely MSNs) induced by D1 receptor agonist SKF-38393 in striatal slices (Arcuri et al., 2018; Marti et al., 2012), a biochemical predictor of anti-dyskinetic activity. In this model, we now show that CCG-203920 potentiates the effect of a submaximal dose of AT-403 without affecting the D1 response alone. Consistently, CCG-203920 potentiated the antidyskinetic effect of AT-403, significantly extending the delay in AIM onset induced by AT-403. Because this effect was not accompanied by the worsening of the positive effect of AT-403 on rotarod performance, it is likely due to a true potentiation of its antidyskinetic properties. Because we show that the same dose of CCG-203920 reversed raclopride-induced akinesia in mice through selective interaction with RGS4, we are confident that also the antidyskinetic effect of CCG-20920 is mediated by RGS4 targeting. To confirm that the effect of CCG-203920 is truly mediated by interference with the molecular pathways underlying LID, CCG-203920 potentiated the inhibition of ERK phosphorylation induced by AT-403. LID is characterized by aberrant enhancement of Gα and Gβγ signalling pathways downstream of the D1 receptor, such as the cAMP/PKA and MAPK cascades (Santini et al., 2007). Specifically, the increased activity along the canonical and non-canonical D1 pathways leads to the phosphorylation of several downstream effectors in striatal direct pathway MSNs, such as the GluR1 subunit of glutamate AMPA receptor and ERK (Pavon et al., 2006; Santini et al., 2007). We previously reported that a dose of AT-403 as high as 0.1 mg·kg^{-1} normalized pERK levels and blunted LID (Arcuri et al., 2018). We now report that a threefold lower dose, ineffective alone, normalized pERK levels when combined with the experimental RGS4 chemical probe CCG-203920, confirming that RGS4 blockade potentiates the ability of a NOP receptor agonist to modulate MAPK pathway changes underlying LID. As far as pGluR1 levels are concerned, AT-403 alone fully inhibited the rise of pGluR1 associated with dyskinesia, which might have precluded further inhibition by CCG-203920. Overall, these data indicate that RGS4 blockade improves the antidyskinetic effect induced by a NOP receptor agonist and the underlying signalling pathways, without amplifying its sedative effects. This suggests that as for δ opioid receptor agonists (Dripps et al., 2017), RGS4 blockade might differentially impact NOP behaviours and perhaps widen the therapeutic window between sedation and pharmacodynamic effects of potent NOP agonists like AT-403.

Interestingly, previous studies indicated the involvement of RGS4 in the pathogenesis of LID, showing that RGS4 blockade induced therapeutic antidyskinetic effects (Ko et al., 2014; Shen et al., 2015). Specifically, chronic treatment with antisense oligonucleotides targeting RGS4 reduced AIM development during L-Dopa priming in a rat model of LID (Ko et al., 2014). Pharmacological blockade of RGS4 is expected to affect GPCRs other than the NOP receptor, inducing off-target effects in brain or neuronal populations not involved in LID. To confirm that an RGS4 inhibitor would selectively target and correct a pathological condition, we show that striatal RGS4 levels are reduced after DA depletion and rapidly up-regulated after L-Dopa administration and dyskinesia onset. This further supports the rationale for therapeutic application of RGS4 inhibitors in LID therapy. Our data confirm previous evidence of reduction of RGS4 expression in DA-depleted animals (Geurts et al., 2003; Ko et al., 2014). More specifically, they nicely complement an ex vivo study in 6-OHDA hemilesioned dyskinetic rats (Ko et al., 2014), where RGS4 expression was found to be reduced in the lesioned striatum after DA depletion and increased following chronic L-Dopa treatment, the increase being more marked at 1 h (i.e., ON L-Dopa) than at 24 h (i.e., OFF L-Dopa) after L-Dopa administration. Surprisingly, however, our study also revealed a reduction in the unlesioned striatum, suggesting a powerful influence of the cortico-basal ganglia-thalamo-cortical loop and/or cross-striatal dopaminergic projections over RGS4 levels.

14765381, 2023, 7, Downloaded from https://bpspubs.onlinelibrary.wiley.com/doi/10.1111/bph.15730 by UNIVERSITA DI PADOVA Centro di Ateneo per le Bib Ca, Wiley Online Library on [13/10/2025]. See the Terms and Conditions (https://onlinelibrary.wiley.com/terms-and-conditions) on Wiley Online Library for rules of use; OA articles are governed by the applicable Creative Commons License

In conclusion, we provide strong evidence of a NOP–RGS4 receptor interaction in a cell line and in native tissues and its relevance for the therapy of LID. CCG-203920 potentiated the antidyskinetic effect of NOP agonists without worsening its primary sedative/hypolocomotor properties, possibly preventing the effects resulting from up-regulation of RGS4 induced by L-Dopa in striatum. RGS4 plays an important role in regulating striatal functions and plasticity under parkinsonian conditions (Lerner & Kreitzer, 2012; Shen et al., 2015). The present study confirms the role of RGS4 in LID (Ko et al., 2014; Shen et al., 2015) and lends support to the therapeutic potential of RGS4 inhibitors in the therapy of neuropsychiatric disorders (Ahlers-Dannen et al., 2020).

ACKNOWLEDGEMENTS

This study was funded by local grants from the University of Ferrara (Università degli Studi di Ferrara) (#FAR1891100). We thank Dr Susanne M. Mumby for generous gift of the RGS4 antibody, and Jeffrey Leipprandt and Behirda Karaj for technical assistance. Open Access Funding provided by Universita degli Studi di Ferrara within the CRUI-CARE Agreement.

AUTHOR CONTRIBUTIONS

Clarissa Anna Pisanò and Michele Morari conceived the study, designed the experiments and drafted the final version of the manuscript. Gerard W. O'Keeffe, Richard R. Neubig and Riccardo Brambilla designed and supervised the experiments in in vitro models. Clarissa Anna Pisanò performed experiments in cell lines and dyskinetic rats. Martina Mazzocchi performed experiments in primary striatal neurons. Daniela Mercatelli performed Western blot analysis. Alberto Brugnoli performed behavioural experiments in RGS4$^{-/-}$ mice. Ilaria Morella and Stefania Fasano performed experiments in mouse slices. Nurulain T. Zaveri critically revised NOP pharmacology and synthesized AT-403. All authors reviewed and edited the manuscript.

CONFLICT OF INTEREST

The authors declare no conflict of interest.

DECLARATION OF TRANSPARENCY AND SCIENTIFIC RIGOUR

This Declaration acknowledges that this paper adheres to the principles for transparent reporting and scientific rigour of preclinical research as stated in the *BJP* guidelines for Design and Analysis, Immunoblotting and Immunochemistry, and Animal Experimentation, and as recommended by funding agencies, publishers and other organizations engaged with supporting research.

DATA AVAILABILITY STATEMENT

The data that support the findings of this study are available from the corresponding author upon reasonable request. Some data may not be made available because of privacy or ethical restrictions.

ORCID

Michele Morari https://orcid.org/0000-0002-4601-4454

REFERENCES

Ahlers-Dannen, K. E., Spicer, M. M., & Fisher, R. A. (2020). RGS proteins as critical regulators of motor function and their implications in Parkinson's disease. *Molecular Pharmacology*, *98*(6), 730–738. https://doi.org/10.1124/mol.119.118836

Alexander, S. P., Christopoulos, A., Davenport, A. P., Kelly, E., Mathie, A., Peters, J. A., Veale, E. L., Armstrong, J. F., Faccenda, E., Harding, S. D., Pawson, A. J., Southan, C., Davies, J. A., Abbracchio, M. P., Alexander, W., Al-Hosaini, K., Bäck, M., Barnes, N. M., Bathgate, R., … Ye, R. D. (2021). The Concise Guide to PHARMACOLOGY 2021/22: G protein-coupled receptors. *British Journal of Pharmacology*, *178*-(Suppl 1), S27–S156.

Alexander, S. P., Kelly, E., Mathie, A., Peters, J. A., Veale, E. L., Armstrong, J. F., Faccenda, E., Harding, S. D., Pawson, A. J., Southan, C., Buneman, O. P., Cidlowski, J. A., Christopoulos, A., Davenport, A. P., Fabbro, D., Spedding, M., Striessnig, J., Davies, J. A., Ahlers-Dannen, K. E., … Zolghadri, Y. (2021). The Concise Guide to PHARMACOLOGY 2021/22: Introduction and other protein targets. *British Journal of Pharmacology*, *178*(Suppl 1), S1–S26. https://doi.org/10.1111/bph.15540

Alexander, S. P. H., Roberts, R. E., Broughton, B. R. S., Sobey, C. G., George, C. H., Stanford, S. C., Cirino, G., Docherty, J. R., Giembycz, M. A., Hoyer, D., Insel, P. A., Izzo, A. A., Ji, Y., MacEwan, D. J., Mangum, J., Wonnacott, S., & Ahluwalia, A. (2018). Goals and practicalities of immunoblotting and immunohistochemistry: A guide for submission to the *British Journal of Pharmacology*. *British Journal of Pharmacology*, *175*(3), 407–411. https://doi.org/10.1111/bph.14112

Arcuri, L., Novello, S., Frassineti, M., Mercatelli, D., Pisano, C. A., Morella, I., Fasano, S., Journigan, B. V., Meyer, M. E., Polgar, W. E., Brambilla, R., Zaveri, N. T., & Morari, M. (2018). Anti-Parkinsonian and anti-dyskinetic profiles of two novel potent and selective nociceptin/orphanin FQ receptor agonists. *British Journal of Pharmacology*, *175*(5), 782–796. https://doi.org/10.1111/bph.14123

Bastide, M. F., Meissner, W. G., Picconi, B., Fasano, S., Fernagut, P. O., Feyder, M., Francardo, V., Alcacer, C., Ding, Y., Brambilla, R., Fisone, G., Jon Stoessl, A., Bourdenx, M., Engeln, M., Navailles, S., de Deurwaerdère, P., Ko, W. K. D., Simola, N., Morelli, M., … Bézard, E. (2015). Pathophysiology of L-dopa-induced motor and non-motor complications in Parkinson's disease. *Progress in Neurobiology*, *132*, 96–168. https://doi.org/10.1016/j.pneurobio.2015.07.002

Berman, D. M., Wilkie, T. M., & Gilman, A. G. (1996). GAIP and RGS4 are GTPase-activating proteins for the Gi subfamily of G protein α subunits. *Cell*, *86*(3), 445–452. https://doi.org/10.1016/S0092-8674(00)80117-8

Blazer, L. L., Storaska, A. J., Jutkiewicz, E. M., Turner, E. M., Calcagno, M., Wade, S. M., Wang, Q., Huang, X. P., Traynor, J. R., Husbands, S. M., Morari, M., & Neubig, R. R. (2015). Selectivity and anti-Parkinson's potential of thiadiazolidinone RGS4 inhibitors. *ACS Chemical Neuroscience*, *6*(6), 911–919. https://doi.org/10.1021/acschemneuro.5b00063

Brugnoli, A., Pisano, C. A., & Morari, M. (2020). Striatal and nigral muscarinic type 1 and type 4 receptors modulate levodopa-induced dyskinesia and striato-nigral pathway activation in 6-hydroxydopamine hemilesioned rats. *Neurobiology of Disease*, *144*, 105044. https://doi.org/10.1016/j.nbd.2020.105044

Buzas, B., Rosenberger, J., & Cox, B. M. (1998). Activity and cyclic AMP-dependent regulation of nociceptin/orphanin FQ gene expression in primary neuronal and astrocyte cultures. *Journal of Neurochemistry*, *71*(2), 556–563. https://doi.org/10.1046/j.1471-4159.1998.71020556.x

Cenci, M. A., & Crossman, A. R. (2018). Animal models of L-dopa-induced dyskinesia in Parkinson's disease. *Movement Disorders*, *33*(6), 889–899. https://doi.org/10.1002/mds.27337

14765381, 2023, 7, Downloaded from https://bpspubs.onlinelibrary.wiley.com/doi/10.1111/bph.15730 by UNIVERSITA DI PADOVA Centro di Ateneo per le Bib Ca, Wiley Online Library on [13/10/2025]. See the Terms and Conditions (https://onlinelibrary.wiley.com/terms-and-conditions) on Wiley Online Library for rules of use; OA articles are governed by the applicable Creative Commons License

Cenci, M. A., Lee, C. S., & Bjorklund, A. (1998). L-DOPA-induced dyskinesia in the rat is associated with striatal overexpression of prodynorphin- and glutamic acid decarboxylase mRNA. *The European Journal of Neuroscience*, *10*(8), 2694–2706. https://doi.org/10.1046/j.1460-9568.1998.00285.x

Cenci, M. A., & Lundblad, M. (2007). Ratings of L-DOPA-induced dyskinesia in the unilateral 6-OHDA lesion model of Parkinson's disease in rats and mice. *Current Protocols in Neuroscience*. Chapter 9: Unit 9 25

Cifelli, C., Rose, R. A., Zhang, H., Voigtlaender-Bolz, J., Bolz, S. S., Backx, P. H., & Heximer, S. P. (2008). RGS4 regulates parasympathetic signaling and heart rate control in the sinoatrial node. *Circulation Research*, *103*(5), 527–535. https://doi.org/10.1161/CIRCRESAHA.108.180984

Curtis, M. J., Alexander, S., Cirino, G., Docherty, J. R., George, C. H., Giembycz, M. A., Hoyer, D., Insel, P. A., Izzo, A. A., Ji, Y., MacEwan, D. J., Sobey, C. G., Stanford, S. C., Teixeira, M. M., Wonnacott, S., & Ahluwalia, A. (2018). Experimental design and analysis and their reporting II: Updated and simplified guidance for authors and peer reviewers. *British Journal of Pharmacology*, *175*(7), 987–993. https://doi.org/10.1111/bph.14153

Dripps, I. J., Wang, Q., Neubig, R. R., Rice, K. C., Traynor, J. R., & Jutkiewicz, E. M. (2017). The role of regulator of G protein signaling 4 in delta-opioid receptor-mediated behaviors. *Psychopharmacology*, *234*(1), 29–39. https://doi.org/10.1007/s00213-016-4432-5

Duty, S., & Jenner, P. (2011). Animal models of Parkinson's disease: A source of novel treatments and clues to the cause of the disease. *British Journal of Pharmacology*, *164*(4), 1357–1391. https://doi.org/10.1111/j.1476-5381.2011.01426.x

Ebert, P. J., Campbell, D. B., & Levitt, P. (2006). Bacterial artificial chromosome transgenic analysis of dynamic expression patterns of regulator of G-protein signaling 4 during development. II. Subcortical regions. *Neuroscience*, *142*(4), 1163–1181. https://doi.org/10.1016/j.neuroscience.2006.08.012

Fasano, S., D'Antoni, A., Orban, P. C., Valjent, E., Putignano, E., Vara, H., Pizzorusso, T., Giustetto, M., Yoon, B., Soloway, P., Maldonado, R., Caboche, J., & Brambilla, R. (2009). Ras-guanine nucleotide-releasing factor 1 (Ras-GRF1) controls activation of extracellular signal-regulated kinase (ERK) signaling in the striatum and long-term behavioral responses to cocaine. *Biological Psychiatry*, *66*(8), 758–768. https://doi.org/10.1016/j.biopsych.2009.03.014

Feng, H., Sjogren, B., Karaj, B., Shaw, V., Gezer, A., & Neubig, R. R. (2017). Movement disorder in GNAO1 encephalopathy associated with gain-of-function mutations. *Neurology*, *89*(8), 762–770. https://doi.org/10.1212/WNL.0000000000004262

Ferrari, F., Malfacini, D., Journigan, B. V., Bird, M. F., Trapella, C., Guerrini, R., Lambert, D. G., Calo', G., & Zaveri, N. T. (2017). In vitro pharmacological characterization of a novel unbiased NOP receptor-selective nonpeptide agonist AT-403. *Pharmacology Research & Perspectives*, *5*(4), e00333. https://doi.org/10.1002/prp2.333

Garzon, J., Rodriguez-Diaz, M., Lopez-Fando, A., & Sanchez-Blazquez, P. (2001). RGS9 proteins facilitate acute tolerance to mu-opioid effects. *The European Journal of Neuroscience*, *13*(4), 801–811. https://doi.org/10.1046/j.0953-816x.2000.01444.x

Geurts, M., Maloteaux, J. M., & Hermans, E. (2003). Altered expression of regulators of G-protein signaling (RGS) mRNAs in the striatum of rats undergoing dopamine depletion. *Biochemical Pharmacology*, *66*(7), 1163–1170. https://doi.org/10.1016/S0006-2952(03)00447-7

Gold, S. J., Ni, Y. G., Dohlman, H. G., & Nestler, E. J. (1997). Regulators of G-protein signaling (RGS) proteins: Region-specific expression of nine subtypes in rat brain. *The Journal of Neuroscience*, *17*(20), 8024–8037. https://doi.org/10.1523/JNEUROSCI.17-20-08024.1997

Gross, J. D., Kaski, S. W., Schmidt, K. T., Cogan, E. S., Boyt, K. M., Wix, K., Schroer, A. B., McElligott, Z. A., Siderovski, D. P., & Setola, V. (2019). Role of RGS12 in the differential regulation of kappa opioid receptor-dependent signaling and behavior. *Neuropsychopharmacology*, *44*(10), 1728–1741. https://doi.org/10.1038/s41386-019-0423-7

Han, M. H., Renthal, W., Ring, R. H., Rahman, Z., Psifogeorgou, K., Howland, D., Birnbaum, S., Young, K., Neve, R., Nestler, E. J., & Zachariou, V. (2010). Brain region specific actions of regulator of G protein signaling 4 oppose morphine reward and dependence but promote analgesia. *Biological Psychiatry*, *67*(8), 761–769. https://doi.org/10.1016/j.biopsych.2009.08.041

Jutkiewicz, E. M., Rice, K. C., Traynor, J. R., & Woods, J. H. (2005). Separation of the convulsions and antidepressant-like effects produced by the delta-opioid agonist SNC80 in rats. *Psychopharmacology*, *182*(4), 588–596. https://doi.org/10.1007/s00213-005-0138-9

Kimple, A. J., Bosch, D. E., Giguere, P. M., & Siderovski, D. P. (2011). Regulators of G-protein signaling and their Gα substrates: Promises and challenges in their use as drug discovery targets. *Pharmacological Reviews*, *63*(3), 728–749. https://doi.org/10.1124/pr.110.003038

Ko, W. K., Martin-Negrier, M. L., Bezard, E., Crossman, A. R., & Ravenscroft, P. (2014). RGS4 is involved in the generation of abnormal involuntary movements in the unilateral 6-OHDA-lesioned rat model of Parkinson's disease. *Neurobiology of Disease*, *70*, 138–148. https://doi.org/10.1016/j.nbd.2014.06.013

Lerner, T. N., & Kreitzer, A. C. (2012). RGS4 is required for dopaminergic control of striatal LTD and susceptibility to parkinsonian motor deficits. *Neuron*, *73*(2), 347–359. https://doi.org/10.1016/j.neuron.2011.11.015

Lilley, E., Stanford, S. C., Kendall, D. E., Alexander, S. P. H., Cirino, G., Docherty, J. R., George, C. H., Insel, P. A., Izzo, A. A., Ji, Y., Panettieri, R. A., Sobey, C. G., Stefanska, B., Stephens, G., Teixeira, M., & Ahluwalia, A. (2020). ARRIVE 2.0 and the *British Journal of Pharmacology*: Updated guidance for 2020. *British Journal of Pharmacology*, *177*(16), 3611–3616. https://doi.org/10.1111/bph.15178

Marti, M., Mela, F., Fantin, M., Zucchini, S., Brown, J. M., Witta, J., di Benedetto, M., Buzas, B., Reinscheid, R. K., Salvadori, S., Guerrini, R., Romualdi, P., Candeletti, S., Simonato, M., Cox, B. M., & Morari, M. (2005). Blockade of nociceptin/orphanin FQ transmission attenuates symptoms and neurodegeneration associated with Parkinson's disease. *The Journal of Neuroscience*, *25*(42), 9591–9601. https://doi.org/10.1523/JNEUROSCI.2546-05.2005

Marti, M., Mela, F., Guerrini, R., Calo, G., Bianchi, C., & Morari, M. (2004). Blockade of nociceptin/orphanin FQ transmission in rat substantia nigra reverses haloperidol-induced akinesia and normalizes nigral glutamate release. *Journal of Neurochemistry*, *91*(6), 1501–1504. https://doi.org/10.1111/j.1471-4159.2004.02843.x

Marti, M., Rodi, D., Li, Q., Guerrini, R., Fasano, S., Morella, I., Tozzi, A., Brambilla, R., Calabresi, P., Simonato, M., Bezard, E., & Morari, M. (2012). Nociceptin/orphanin FQ receptor agonists attenuate L-DOPA-induced dyskinesias. *The Journal of Neuroscience*, *32*(46), 16106–16119. https://doi.org/10.1523/JNEUROSCI.6408-11.2012

Mercatelli, D., Bezard, E., Eleopra, R., Zaveri, N. T., & Morari, M. (2020). Managing Parkinson's disease: Moving ON with NOP. *British Journal of Pharmacology*, *177*(1), 28–47. https://doi.org/10.1111/bph.14893

Neal, C. R. Jr., Mansour, A., Reinscheid, R., Nothacker, H. P., Civelli, O., Akil, H., & Watson, S. J. Jr. (1999). Opioid receptor-like (ORL1) receptor distribution in the rat central nervous system: Comparison of ORL1 receptor mRNA expression with (125)I-[(14)Tyr]-orphanin FQ binding. *The Journal of Comparative Neurology*, *412*(4), 563–605. https://doi.org/10.1002/(SICI)1096-9861(19991004)412:4%3C563::AID-CNE2%3E3.0.CO;2-Z

Olianas, M. C., Dedoni, S., Boi, M., & Onali, P. (2008). Activation of nociceptin/orphanin FQ-NOP receptor system inhibits tyrosine hydroxylase phosphorylation, dopamine synthesis, and dopamine D (1) receptor signaling in rat nucleus accumbens and dorsal striatum. *Journal of Neurochemistry*, *107*(2), 544–556. https://doi.org/10.1111/j.1471-4159.2008.05629.x

14765381, 2023, 7, Downloaded from https://bpspubs.onlinelibrary.wiley.com/doi/10.1111/bph.15730 by UNIVERSITA DI PADOVA Centro di Ateneo per le Bib Ca, Wiley Online Library on [13/10/2025]. See the Terms and Conditions (https://onlinelibrary.wiley.com/terms-and-conditions) on Wiley Online Library for rules of use; OA articles are governed by the applicable Creative Commons License

Ouimet, C. C., Miller, P. E., Hemmings, H. C. Jr., Walaas, S. I., & Greengard, P. (1984). DARPP-32, a dopamine- and adenosine 3′:5′-monophosphate-regulated phosphoprotein enriched in dopamine-innervated brain regions. III. Immunocytochemical localization. *Journal of Neuroscience*, *4*(1), 111–124.

Paolone, G., Brugnoli, A., Arcuri, L., Mercatelli, D., & Morari, M. (2015). Eltoprazine prevents levodopa-induced dyskinesias by reducing striatal glutamate and direct pathway activity. *Movement Disorders*, *30*(13), 1728–1738. https://doi.org/10.1002/mds.26326

Papale, A., Morella, I. M., Indrigo, M. T., Bernardi, R. E., Marrone, L., Marchisella, F., Brancale, A., Spanagel, R., Brambilla, R., & Fasano, S. (2016). Impairment of cocaine-mediated behaviours in mice by clinically relevant Ras-ERK inhibitors. *eLife*, 5, e17111.

Pavon, N., Martin, A. B., Mendialdua, A., & Moratalla, R. (2006). ERK phosphorylation and FosB expression are associated with L-DOPA-induced dyskinesia in hemiparkinsonian mice. *Biological Psychiatry*, *59*(1), 64–74. https://doi.org/10.1016/j.biopsych.2005.05.044

Paxinos, G., & Watson, C. (1986). *The rat brain in stereotaxic coordinates* (2nd ed.). Academic Press.

Percie du Sert, N., Hurst, V., Ahluwalia, A., Alam, S., Avey, M. T., Baker, M., Browne, W. J., Clark, A., Cuthill, I. C., Dirnagl, U., Emerson, M., Garner, P., Holgate, S. T., Howells, D. W., Karp, N. A., Lazic, S. E., Lidster, K., MacCallum, C. J., Macleod, M., … Würbel, H. (2020). The ARRIVE guidelines 2.0: Updated guidelines for reporting animal research. *British Journal of Pharmacology*, *177*(16), 3617–3624. https://doi.org/10.1111/bph.15193

Pisanò, C. A., Brugnoli, A., Novello, S., Caccia, C., Keywood, C., Melloni, E., Vailati, S., Padoani, G., & Morari, M. (2020). Safinamide inhibits in vivo glutamate release in a rat model of Parkinson's disease. *Neuropharmacology*, *167*, 108006. https://doi.org/10.1016/j.neuropharm.2020.108006

Psifogeorgou, K., Papakosta, P., Russo, S. J., Neve, R. L., Kardassis, D., Gold, S. J., & Zachariou, V. (2007). RGS9-2 is a negative modulator of μ-opioid receptor function. *Journal of Neurochemistry*, *103*(2), 617–625. https://doi.org/10.1111/j.1471-4159.2007.04812.x

Runne, H., Regulier, E., Kuhn, A., Zala, D., Gokce, O., Perrin, V., Sick, B., Aebischer, P., Deglon, N., & Luthi-Carter, R. (2008). Dysregulation of gene expression in primary neuron models of Huntington's disease shows that polyglutamine-related effects on the striatal transcriptome may not be dependent on brain circuitry. *The Journal of Neuroscience*, *28*(39), 9723–9731. https://doi.org/10.1523/JNEUROSCI.3044-08.2008

Sakloth, F., Polizu, C., Bertherat, F., & Zachariou, V. (2020). Regulators of G protein signaling in analgesia and addiction. *Molecular Pharmacology*, *98*, 739–750. https://doi.org/10.1124/mol.119.119206

Santini, E., Valjent, E., Usiello, A., Carta, M., Borgkvist, A., Girault, J. A., Herve, D., Greengard, P., & Fisone, G. (2007). Critical involvement of cAMP/DARPP-32 and extracellular signal-regulated protein kinase signaling in L-DOPA-induced dyskinesia. *The Journal of Neuroscience*, *27*(26), 6995–7005. https://doi.org/10.1523/JNEUROSCI.0852-07.2007

Schmidt, E. R., Morello, F., & Pasterkamp, R. J. (2012). Dissection and culture of mouse dopaminergic and striatal explants in three-dimensional collagen matrix assays. *Journal of Visualized Experiments: JoVE*, *61*, 3691.

Schwarting, R. K., & Huston, J. P. (1996). The unilateral 6-hydroxydopamine lesion model in behavioral brain research. Analysis of functional deficits, recovery and treatments. *Progress in Neurobiology*, *50*(2–3), 275–331. https://doi.org/10.1016/S0301-0082(96)00040-8

Senese, N. B., Kandasamy, R., Kochan, K. E., & Traynor, J. R. (2020). Regulator of G-protein signaling (RGS) protein modulation of opioid receptor signaling as a potential target for pain management. *Frontiers in Molecular Neuroscience*, *13*, 5. https://doi.org/10.3389/fnmol.2020.00005

Shen, W., Plotkin, J. L., Francardo, V., Ko, W. K., Xie, Z., Li, Q., Fieblinger, T., Wess, J., Neubig, R. R., Lindsley, C. W., Conn, P. J., Greengard, P., Bezard, E., Cenci, M. A., & Surmeier, D. J. (2015). M4 muscarinic receptor signaling ameliorates striatal plasticity deficits in models of L-DOPA-induced dyskinesia. *Neuron*, *88*(4), 762–773. https://doi.org/10.1016/j.neuron.2015.10.039

Sjogren, B. (2017). The evolution of regulators of G protein signalling proteins as drug targets—20 years in the making: IUPHAR review 21. *British Journal of Pharmacology*, *174*(6), 427–437. https://doi.org/10.1111/bph.13716

Stratinaki, M., Varidaki, A., Mitsi, V., Ghose, S., Magida, J., Dias, C., Russo, S. J., Vialou, V., Caldarone, B. J., Tamminga, C. A., Nestler, E. J., & Zachariou, V. (2013). Regulator of G protein signaling 4 [corrected] is a crucial modulator of antidepressant drug action in depression and neuropathic pain models. *Proceedings of the National Academy of Sciences of the United States of America*, *110*(20), 8254–8259. https://doi.org/10.1073/pnas.1214696110

Tesmer, J. J., Berman, D. M., Gilman, A. G., & Sprang, S. R. (1997). Structure of RGS4 bound to AlF4--activated $G_{i\alpha1}$: Stabilization of the transition state for GTP hydrolysis. *Cell*, *89*(2), 251–261. https://doi.org/10.1016/S0092-8674(00)80204-4

Toll, L., Bruchas, M. R., Calo, G., Cox, B. M., & Zaveri, N. T. (2016). Nociceptin/orphanin FQ receptor structure, signaling, ligands, functions, and interactions with opioid systems. *Pharmacological Reviews*, *68*(2), 419–457. https://doi.org/10.1124/pr.114.009209

Traynor, J. (2012). μ-Opioid receptors and regulators of G protein signaling (RGS) proteins: From a symposium on new concepts in mu-opioid pharmacology. *Drug and Alcohol Dependence*, *121*(3), 173–180. https://doi.org/10.1016/j.drugalcdep.2011.10.027

Traynor, J. R., & Neubig, R. R. (2005). Regulators of G protein signaling & drugs of abuse. *Molecular Interventions*, *5*(1), 30–41. https://doi.org/10.1124/mi.5.1.7

Turner, E. M., Blazer, L. L., Neubig, R. R., & Husbands, S. M. (2012). Small molecule inhibitors of regulator of G protein signalling (RGS) proteins. *ACS Medicinal Chemistry Letters*, *3*(2), 146–150. https://doi.org/10.1021/ml200263y

Viaro, R., Sanchez-Pernaute, R., Marti, M., Trapella, C., Isacson, O., & Morari, M. (2008). Nociceptin/orphanin FQ receptor blockade attenuates MPTP-induced parkinsonism. *Neurobiology of Disease*, *30*(3), 430–438. https://doi.org/10.1016/j.nbd.2008.02.011

Xie, G. X., Yanagisawa, Y., Ito, E., Maruyama, K., Han, X., Kim, K. J., Han, K. R., Moriyama, K., & Palmer, P. P. (2005). N-terminally truncated variant of the mouse GAIP/RGS19 lacks selectivity of full-length GAIP/RGS19 protein in regulating ORL1 receptor signaling. *Journal of Molecular Biology*, *353*(5), 1081–1092. https://doi.org/10.1016/j.jmb.2005.09.040

Zachariou, V., Georgescu, D., Sanchez, N., Rahman, Z., DiLeone, R., Berton, O., Neve, R. L., Sim-Selley, L. J., Selley, D. E., Gold, S. J., & Nestler, E. J. (2003). Essential role for RGS9 in opiate action. *Proceedings of the National Academy of Sciences of the United States of America*, *100*(23), 13656–13661. https://doi.org/10.1073/pnas.2232594100

SUPPORTING INFORMATION

Additional supporting information may be found in the online version of the article at the publisher's website.

How to cite this article: Pisanò, C. A., Mercatelli, D., Mazzocchi, M., Brugnoli, A., Morella, I., Fasano, S., Zaveri, N. T., Brambilla, R., O'Keeffe, G. W., Neubig, R. R., & Morari, M. (2023). Regulator of G-Protein Signalling 4 (RGS4) negatively modulates nociceptin/orphanin FQ opioid receptor signalling: Implication for L-Dopa-induced dyskinesia. *British Journal of Pharmacology*, *180*(7), 927–942. https://doi.org/10.1111/bph.15730

14765381, 2023, 7, Downloaded from https://bpspubs.onlinelibrary.wiley.com/doi/10.1111/bph.15730 by UNIVERSITA DI PADOVA Centro di Ateneo per le Bib Ca, Wiley Online Library on [13/10/2025]. See the Terms and Conditions (https://onlinelibrary.wiley.com/terms-and-conditions) on Wiley Online Library for rules of use; OA articles are governed by the applicable Creative Commons License